Global NEST Journal, Vol 28, No 2, 07789

CCER valuation under emission uncertainty: a dual framework of compliance optimization and regime-switching GBM

Hua Tang[1,2], Yue Liu[3], Jiayi Wang[3]*, Jiawen Liu[3], Wangfei Luo[4], Tianbai Wang[5]
1 School of Management, Jiangsu University, Zhenjiang, 212013, Jiangsu, PR China.
2 Business School of Wenzhou University, Wenzhou City, 325035, Zhejiang, PR China; PR China
3 School of Finance and Economics, Jiangsu University, Zhenjiang, 212013, Jiangsu, PR China
4 School of Electrical and Information Engineering, Jiangsu University, Zhenjiang 212013, PR China
5 China School of Banking and Finance UIBE, University of International Business and Economics, Beijing,100029, PR China
Supported by the grant from the Major Program of the National Social Science Fund of China (22&ZD136).
Received: 25/06/2025, Accepted: 10/01/2026, Available online: 27/01/2026
*to whom all correspondence should be addressed: e-mail: 15139253806@163.com
https://doi.org/10.30955/gnj.07789

Graphical abstract

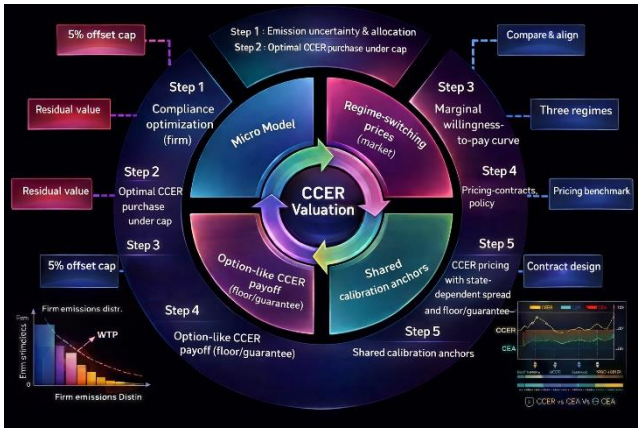

Abstract

This paper develops an integrated framework to value China Certified Emission Reductions (CCER) in the context of the national emissions trading system. At the micro level, we refine the income approach by endogenizing firms' CCER purchase decisions under emission uncertainty, offset caps and residual value risk, deriving a closed-form marginal willingness-to-pay schedule linked to firm-specific emission distributions, allowance allocations and policy parameters. At the macro level, we model carbon prices with a three-regime switching geometric Brownian motion calibrated to Beijing carbon market and electricity data, and price CCER as a real-option-like asset with state-dependent CEA-CCER spreads and guarantee-type payoffs. Comparing the two layers, we show how income-based benchmarks and regime-switching option values differ yet can be aligned to inform CCER pricing, contract design and policy reform in China's carbon market.

Keywords: CCER valuation; Carbon assets; Income approach; Regime-switching GBM; Real options.

1. Introduction

China's national carbon emission trading system incorporates the China Certified Emission Reduction (CCER) mechanism as a key supplementary instrument for achieving carbon peaking and neutrality targets at reduced costs. Regulated enterprises may substitute CCER for Carbon Emission Allowances (CEA) up to specified proportions when offsetting verified emissions, which should in theory lower aggregate abatement costs while channeling investment toward low-carbon projects. Yet CCER's actual economic value emerges from the interplay of multiple factors: firm-level emission uncertainty, quota allocation methodologies, caps on offsetting ratios, policy-driven sunset clauses governing CCER eligibility, and carbon market prices that swing with macroeconomic cycles and regulatory shifts. These institutional and market features reveal that CCER functions neither as a riskless compliance instrument nor as a straightforward derivative of CEA prices; both enterprises and regulators require valuation frameworks capable of reconciling micro-level compliance incentives with macro-level price movements.

Current CCER valuation practices display fragmentation across two dimensions. Income approach studies concentrate on the expected cost savings CCER delivers relative to CEA, yet these analyses commonly take CCER purchase volumes as given and overlook maturity and residual value risks, thereby constraining their capacity to represent firms' actual procurement decisions under uncertainty. Market approach studies deploy stochastic models for carbon prices but frequently treat CCER as a scaled replica of CEA, failing to explicitly embed compliance constraints, offset ratios, or policy validity windows. A disconnect has thus emerged between enterprise-centered analysis that proves intuitive but

Hua Tang, Yue Liu, Jiayi Wang, Jiawen Liu, Wangfei Luo, Tianbai Wang (2026), CCER valuation under emission uncertainty: a dual framework of compliance optimization and regime-switching GBM, *Global NEST Journal*, **28**(2), 07789.

static and market-centered modeling that remains dynamic yet weakly anchored to the compliance architecture. This paper seeks to close that gap by developing an integrated framework: it merges a micro-level income approach grounded in firms' optimal CCER demand with a macro-level market approach that captures CEA and CCER price evolution via regime switching (Hussain *et al.* 2021) and geometric Brownian motion (Li, W. *et al.* 2021; Liu, Y. *et al.*, 2023a; Liu, Y. *et al.* 2023b), pricing CCER as a real-option-like asset.

From this integrated perspective, the paper advances three principal innovations. First, at the micro level, it refines the income approach by endogenizing CCER purchase quantities as solutions to compliance cost minimization problems under stochastic emissions, regulatory ceilings, and uniform residual values. This yields a closed-form marginal willingness-to-pay curve that directly links firm-specific emission distributions, quota allocations, and policy parameters to CCER valuation. Second, at the macro level, the paper introduces a three-state regime-switching geometric Brownian motion model calibrated using Beijing carbon market data and electricity consumption growth patterns. It jointly models CEA and CCER prices under regime-dependent drift rates, volatilities, and spread ratios, valuing CCER through discounted risk-neutral expectations based on guarantee-type payoffs that reflect compliance substitutability and residual value floors. Third, the paper juxtaposes micro- and macro-level findings, employing shared calibration inputs such as expected CEA settlement prices and CCER residual values to conduct a consistent cross-comparison of valuation outcomes. Results demonstrate that the income approach's benchmark value and regime-switching real option valuation together furnish a foundation for CCER pricing, contract design, and policy formulation.

2. Literature review

We take the literature review via two aspects, one is about carbon asset, another is about asset pricing especially for intangible assets.

2.1. Review on the researches about carbon asset

Recent work on carbon assets has started to connect climate policy, corporate decision-making, and financial market behavior, shedding light on both transition risks and emerging valuation challenges. Research at the sectoral and policy level shows that concentrated ownership of power-sector assets vulnerable to stranding creates vested interests capable of slowing or blocking ambitious climate measures, pointing to governance obstacles and distributional tensions in decarbonization pathways (Chevallier *et al.* 2021; von Dulong 2023). Analyses of corporate carbon footprints across complete value chains find that embedded emissions in listed firms vary dramatically between upstream and downstream operations, altering how investors assess risk exposure and meet disclosure obligations (Langley *et al.* 2021; Zhang *et al.* 2023). Firm-level data indicate that equity markets now price corporate carbon emissions more systematically, with valuations reflecting both total emissions and the perceived credibility of decarbonization plans (Zhang 2025; Chen and Lai 2025). On the asset-pricing front, researchers increasingly model carbon allowances and credits as contingent claims: option frameworks price carbon assets and support digital tools for dynamic hedging and project evaluation (Liu et al. 2022), while real-options techniques measure the economic value of operational choices such as continuing or shutting down emission-intensive power plants under tightening carbon limits (Liu *et al.* 2021). Where macro-finance meets climate, carbon pricing emerges as a driver of structural change toward greener growth trajectories, redirecting capital flows from high-carbon sectors (Langley *et al.* 2021; Mengesha and Roy 2025), yet climate and policy uncertainty propagate forcefully across energy and carbon markets, with asymmetric causal connections running among economic policy uncertainty, oil price volatility, clean energy indices, carbon futures and green bonds (Wang X. *et al.* 2022; Siddique *et al.* 2023). Empirical studies further reveal pronounced spillovers linking fossil fuel, renewable and carbon markets during overlapping climate and energy shocks, implying that carbon assets sit within larger energy-finance networks rather than standing alone (Su *et al.* 2023; Dong and Yoon 2023). Meanwhile, the relaunch of China's CCER market has spurred methodological and project-level advances: feasibility assessments of methane-reduction approaches in oil and gas production highlight a new category of carbon assets with substantial mitigation leverage (Wang *et al.* 2025), and integrated carbon asset management platforms and trading tactics seek to help listed enterprises revalue assets and pursue sustainable development goals (Chen and Lai 2025). Taken together, these studies suggest that carbon assets are shifting from a narrow compliance tool into a diverse financial and strategic asset class whose worth hinges on policy architecture, technology trajectories, cross-market linkages and firm-level organizational capacity (Chevallier *et al.* 2021; Liu *et al.* 2022; Mengesha and Roy 2025). Beyond energy and finance, valuation-relevant impacts of carbon-related assets and practices now extend into material-production industries including agriculture and chemicals, covering soil carbon sequestration, inorganic soil carbon behavior, and biochar-derived carbon materials (Nazir *et al.* 2023; Raza *et al.* 2024; Mahmood *et al.* 2025).

2.2. Review on the researches about intangible asset pricing

A growing body of research on intangible asset pricing examines how non-physical drivers such as information, expectations, environmental performance and intellectual capital increasingly shape asset values. At the measurement and reporting level, surveys and meta-analyses point to persistent gaps between the economic significance of intangibles and their treatment in financial statements, documenting conceptual and empirical obstacles in valuing items such as R&D, data, and organizational capital (Van Criekingen *et al.* 2022; Jeny

and Moldovan 2022; Barker *et al.* 2022). Firm-level studies build on these observations to show that intangible resources can forecast future performance and ought to be priced by investors, with deep learning models extracting value-relevant signals from complex intangible asset profiles (Pechlivanidis *et al.* 2022). Related work broadens the concept of intangibles to include environmental attributes: carbon emissions and carbon risk enter asset pricing models as non-traditional factors, with mounting evidence that emissions and climate exposures affect stock returns and capital costs, especially in emerging markets (van Benthem *et al.* 2022; Wang H. *et al.* 2022; Bolton and Kacperczyk 2024). Time-varying investor preferences for green attributes and evolving policy signals further influence how environmental performance gets rewarded in asset prices, suggesting that such performance has itself become a priced intangible (Dutta 2022; Alessi *et al.* 2023). Where macro-policy meets asset valuation, studies of risk-adjusted carbon prices and retrospective evaluations of carbon pricing schemes reveal that expectations about future regulation and abatement costs embed themselves into long-run asset values, effectively converting regulatory trajectories into a form of priced intangible risk (Van den Bremer and Van der Ploeg 2021; Green, 2021). On the methodological front, advances in behavioral and computational finance demonstrate that even nominal price illusions and data monetization practices introduce new intangible dimensions into pricing: behavioral biases in nominal valuation distort asset prices in ways traditional factors miss, while datasets themselves become tradable intangible assets whose prices can be learned via deep learning-based monetization frameworks (Yang and Yang, 2022; Hao *et al.*, 2025). Taken together, this literature argues that modern asset pricing must systematically incorporate a wide spectrum of intangibles spanning accounting-based intellectual capital, proprietary data, environmental quality and policy expectations, deploying richer models and machine learning techniques to connect these largely off-balance-sheet attributes to observed returns (Van Criekingen *et al.*, 2022; Pechlivanidis *et al.*, 2022; Alessi *et al.*, 2023).

These studies collectively demonstrate that carbon assets and other intangibles are increasingly priced through their interactions with policy, firm behavior and market expectations, yet existing research tends to separate micro compliance analyses from macro market models. Drawing on these insights, this paper treats CCER as a carbon-related intangible asset and constructs an integrated valuation framework that connects optimal firm-level CCER demand under emission and policy uncertainty with regime-switching GBM-based pricing of CEA and CCER, bridging income-based and market-based perspectives to inform CCER pricing, contract design and policy.

3. Micro-level CCER valuation:from the firms' perspective

3.1. Theoretical analysis and model construction

This section constructs an improved CCER valuation model grounded in optimal enterprise purchasing decisions under emission uncertainties, regulatory constraints, and policy-induced invalidation risk. Unlike earlier discrete and continuous distribution models where CCER quantity enters exogenously and unit value represents average cost savings per ton, the present framework endogenizes purchased CCER quantity as the solution to a cost minimization problem and derives the associated willingness to pay as a theoretically grounded estimate of marginal value. This approach preserves the intuitive cost-difference logic inherent in the income method while directly tying CCER value to firm-specific emission risk, incorporating residual value and the potential for excess CCER to lose validity after the compliance window, and permitting heterogeneous enterprise characteristics such as size, quota allocation and volatility to generate differentiated CCER valuations.

We consider a representative compliance enterprise *i* facing uncertain annual carbon emissions in the target year (for instance, 2024). Let *E* denote its random annual emissions (tonnes of CO2 equivalent). Consistent with the empirical setting in the previous section, *E* is modeled from historical data (2017–2023) and is assumed to follow a continuous distribution with mean μ_E and variance σ_E^2, with cumulative distribution function $F_E(\cdot)$ well-defined;in applications a normal or lognormal specification can be used, or an empirically estimated non-parametric distribution.

The enterprise holds or expects to receive an annual allocation of carbon emission allowances (CEA) denoted by *A*, and may purchase a quantity *Q* of CCER to offset emissions in the same compliance period. The maximum proportion of emissions that can be offset with CCER is capped at α (5% in the Chinese system), which implies an upper bound $Q \le Q^{max}$, where Q^{max} can be set as $\alpha\mu_E$ or, more conservatively, as $\alpha(\mu_E+z\sigma_E)$ for a chosen safety quantile *z*. Throughout the analysis we treat *Q* as a continuous decision variable in [0, Q^{max}].

At the beginning of the compliance period (or at an intermediate time before the deadline), the firm chooses *Q* and pays p_cQ, where p_c is the unit market price of CCER. We assume that the CEA price at the time of final compliance is stochastic but that the firm can form an expectation $\bar{p}_A$ of the average marginal cost of acquiring additional CEA close to the settlement date, inferred from historical trading data or from a separate market-approach model (e.g., GBM or LSTM). The regulatory frame-work typically stipulates a penalty F per tonne of uncovered emissions; for analytic clarity we assume $F \ge \bar{p}_A$, so that a rational firm will always purchase CEA to achieve full coverage before paying penalties, and compliance behavior can be summarized as 'buy CEA until the emission shortfall is fully covered'.

Given a realization of E, the firm's compliance balance at the end of the period is *A*+*Q*. If *E* > *A*+*Q* , the firm must purchase additional CEA on the spot market to cover the

shortfall *E*–*A*–*Q* at expected marginal cost $\bar{p}_A(E-A-Q)$, ignoring second-order price feedback from individual trades. If instead *E*<*A*+*Q*, the firm ends the period with surplus compliance assets $A+Q-E$. Because CCER eligibility in the Chinese national trading system is subject to strict temporal limitations (for example, credits registered before March 14, 2017 are usable only until December 31, 2024 and CCER trading effectively ceases after the compliance submission deadline), surplus CCER face significant expiration and liquidity risks, whereas surplus CEA generally remain valid and tradable in subsequent periods or can be sold back to the market.

To capture these asymmetries while keeping the model tractable, we postulate that surplus compliance assets at the end of the period are valued at a residual price v_C^{res}. A more detailed specification could distinguish between surplus CEA and CCER, for example assigning CEA a residual value close to $\bar{p}_A$ and CCER a value $(1-\theta)\lambda p_C$ based on a survival probability (1–θ) and a resale discount factor $\lambda \in [0,1]$ in voluntary markets. For parsimony, we aggregate these effects into a single effective residual value v_C^{res}, interpreted as the expected liquidation value per tonne of surplus compliance asset, net of policy invalidation and market illiquidity; typically $v_C^{res} < \bar{p}_A$ and, for CCER approaching their sunset date, it can be substantially lower.

Under these assumptions, for a given CCER purchase quantity Q and a particular realization of emissions *E*, the firm's random total cost of compliance can be written as

$$\mathrm{TC}(Q;E) = p_C Q + \bar{p}_A(E-A-Q)_+ - v_C^{res}(A+Q-E)_+ \tag{3.1}$$

where $(x)_+ = \max\{x, 0\}$ Here $p_C Q$ is the certain upfront cost of purchasing *Q* tonnes of CCER, $\bar{p}_A(E-A-Q)_+$ is the cost of "filling the gap with CEA" when realized emissions exceed *A*+*Q*, and $-v_C^{res}(A+Q-E)_+$ reflects the residual value of surplus compliance assets when *E*<*A*+*Q*

Given CCER purchase quantity *Q*, the firm's expected total compliance cost is

$$\mathrm{E}\left[\mathrm{TC}(Q;E)\right] = p_C Q + \mathrm{E}\left[\bar{p}_A(E-A-Q)_+\right] - \mathrm{E}\left[v_C^{\mathrm{res}}(A+Q-E)_+\right], \tag{3.2}$$

where the expectation is taken over $E \sim f_E(e)$. The firm's decision problem is

$$Q^* = \arg\min_{0\le Q\le Q^{\max}} \mathrm{E}\left[\mathrm{TC}(Q;E)\right], \tag{3.3}$$

which formalizes, within the income-approach framework, the strategic decision of 'how many CCER to buy' under emission and price uncertainty.

To derive the first-order condition for an interior solution, differentiate (3.2) with respect to *Q*. Since TC(*Q*; *E*) depends on *Q* only through $p_c Q$ and the positive-part terms, and $(E-A-Q)_+$, $(A+Q-E)_+$ are almost everywhere differentiable in *Q* ,we have $\frac{\partial}{\partial Q}(E-A-Q)_+ = -1_{\{E>A+Q\}}$ and $\frac{\partial}{\partial Q}(A+Q-E)_+ = 1_{\{E<A+Q\}}$, where $1_{\{\cdot\}}$ denotes the indicator function. Substituting and using linearity of expectation gives

$$\frac{d}{dQ}\mathrm{E}\left[\mathrm{TC}(Q;E)\right] = p_C + \mathrm{E}\left[-\bar{p}_A 1_{\{E>A+Q\}} - v_C^{res} 1_{\{E<A+Q\}}\right] = p_C - \bar{p}_A \mathrm{P}(E>A+Q) - v_C^{res}\mathrm{P}(E<A+Q), \tag{3.4}$$

where we used $\mathrm{E}\left[1_{\{E>A+Q\}}\right] = \mathrm{P}(E>A+Q)$ and $\mathrm{E}\left[1_{\{E<A+Q\}}\right] = \mathrm{P}(E<A+Q)$. The second term represents the expected marginal saving in CEA "gap-filling" cost, and the third term captures the change in expected residual value from buying one more tonne of CCER.

Setting (3.4) equal to zero at *Q** yields

$$p_C = \bar{p}_A \mathrm{P}\left(E>A+Q^*\right) + v_C^{res}\mathrm{P}\left(E<A+Q^*\right). \tag{3.5}$$

For a continuous emission distribution we have $\mathrm{P}\left(E>A+Q^*\right) + \mathrm{P}\left(E<A+Q\right) \approx 1$.

Rearranging (3.5) gives the key pricing relation

$$\underbrace{p_C}_{\substack{\text{CCER unit price at Q*}\\ \text{(marginal willingness-to-pay)}}} = \underbrace{v_C^{\mathrm{res}}}_{\substack{\text{residual value bencgmark}\\ \text{when CCER mainly end as surplus}}} + \underbrace{\bar{p}_A v_C^{\mathrm{res}}}_{\substack{\text{compliance−use premium}\\ \text{over pure residual value}}} \underbrace{P(E>A+Q^*)}_{\substack{\text{proability of an emission short all}\\ \text{after buying Q* tonnes of CCER}}} \tag{3.6}$$

The marginal willingness-to-pay at *Q** is thus a weighted average of the expected marginal CEA cost $\bar{p}_A$ and the residual value v_C^{res}, with the weight on $\bar{p}_A$ given by the shortfall probability $\mathrm{P}\left(E>A+Q^*\right)$. When this probability is high, p_c is close to $\bar{p}_A$; when it is low, p_c moves toward v_C^{res}.

To obtain an explicit pricing formula, assume $E \sim \mathrm{N}\left(\mu_E, \sigma_E^2\right)$, with ($\mu_E$, σ_E) estimated from historical firm-level data. The shortfall probability can then be expressed via the standard normal CDF Φ(·) as

$$\mathrm{P}\left(E>A+Q\right) = 1-\Phi\left(\frac{A+Q-\mu_E}{\sigma_E}\right). \tag{3.7}$$

Substituting (3.7) into (3.6) yields the central CCER price-quantity relation

$$\underbrace{\mathrm{P}^*_{\mathrm{C}}(Q)}_{\substack{\text{firm-level marinal}\\ \text{(willingness-to-pay at Q)}}} = \underbrace{v_C^{\mathrm{res}}}_{\substack{\text{residual value}\\ \text{surplus states}}} + \underbrace{\bar{\mathrm{p}}_{\mathrm{A}} v_{\mathrm{C}}^{\mathrm{res}}}_{\substack{\text{incremental value of CCER}\\ \text{as a compliance instrument}}} \underbrace{[1-\Phi(\frac{A+Q-\mu_E}{\sigma_E})]}_{\substack{\text{proability of a shortfall}\\ \text{after buying Q tonnes of CCER}}} \tag{3.8}$$

For small *Q* such that $A+Q \ll \mu_E$, the standardized term $(A+Q-\mu_E)/\sigma_E$ is very negative, Φ(·) is close to 0, and the

shortfall probability is close to 1, so $p_C^*(Q) \approx \bar{p}_A$ and CCER are almost fully valued at the expected marginal CEA price; as *Q* increases and *A*+*Q* approaches or exceeds μ_E, the shortfall probability declines and $p_C^*(Q)$ decreases smoothly from $\bar{p}_A$ toward v_C^{res}, reflecting the transition from 'insurance against costly shortfalls' to 'potentially stranded surplus assets'.

Thus, (3.8) can be interpreted as a firm-level demand curve for CCER: for each $Q \in [0, Q^{\max}]$, it gives the marginal price that leaves the firm indifferent between buying an additional tonne of CCER and relying instead on spot CEA purchases or accepting surplus risk. Coupled with (3.3), the most relevant income-based valuations at the firm level are $p_C^*(Q^*)$ (marginal value at the optimum) and $p_C^*(Q^{\max})$ (marginal value when the regulatory offset ratio is fully used). Aggregating such firm-specific marginal values, for example via emission-weighted averages, yields a market-level theoretical CCER price range under the improved income-approach framework.

In implementation: (1) For each firm, estimate (μ_E, σ_E) from historical emissions and determine its expected allowance allocation *A* under national ETS rules, then compute $Q^{max}=\alpha\mu_E$. (2) Specify $\bar{p}_A$ from observed or modeled CEA prices at compliance, and calibrate v_C^{res} using policy information on CCER validity and expected liquidity. (3) For each *Q* on a grid in $[0, Q^{max}]$, compute $\mathrm{P}(E > A+Q)$ via (3.7) and then $p_C^*(Q)$ via (3.8). (4) Solve (3.3) for *Q**, obtain $p_C^*(Q^*)$ or $p_C^*(Q^{max})$, and aggregate across firms to form a market reference price.

3.2. Numerical implementation and discussion on the results

The numerical implementation proceeds as follows (the Matlab implementation for the income-approach model is provided in Appendix B). The model first sets the key global parameters $\alpha = 0.05, \bar{p}_A = 115\ \mathrm{CNY/t}$ and $v_{res} = 30\ \mathrm{CNY/t}$, where α is the maximum CCER offset ratio, $\bar{p}_A$ is the expected marginal CEA settlement price, and v_{res} is the residual (floor) value of CCER. Historical daily CEA and CCER prices from the Word file are read into the program but are used only as background, while the pricing model itself is calibrated directly using the fixed values of $\bar{p}_A$ and v_{res}.

Firm-level emission data are then imported separately for low-emission firms (**Table 2**) and normal-emission firms (**Table 3**). For each firm, the Appendix A provides E_{upper}, E_{mid} and E_{lower} for annual emissions. The code sets $\mu_E = E_{mid}$ as the firm's expected emissions and, assuming (E_{lower}, E_{upper}) is roughly a 90% confidence interval, approximates the standard deviation by $\sigma_E \approx (E_{upper} - E_{lower})/(2z_{0.95})$ with $z_{0.95} \approx 1.64$, imposing $\sigma_E \geq 10^{-6}$ to avoid degeneracy. The allowance allocation is set equal to expected emissions, $A=\mu_E$, and the maximum CCER usage is $Q_{max} = \alpha\mu_E$.

Based on these inputs, the firm-specific marginal willingness-to-pay function for CCER is implemented as

$$p_C^*(Q) = v_{res} + (\bar{p}_A - v_{res})\left[1 - \Phi\left(\frac{A+Q-\mu_E}{\sigma_E}\right)\right]$$

where $\Phi(\cdot)$ is the standard normal cumulative distribution function. In the code this is written as a vectorized anonymous function *pc_fun* using *normcdf*. For each firm, the program evaluates $p_C^*(Q)$ at $Q=0, Q=Q_{max}$ and $Q=Q^*$, where *Q** is obtained by minimizing the expected total compliance cost over $Q \in [0, Q_{max}]$,

$$\mathrm{E}[\mathrm{TC}(Q;E)] = p_C^*(Q)Q + \bar{p}_A \mathrm{E}[(E-T)_+] - v_{res}\mathrm{E}[(T-E)_+], T = A+Q,$$

with $(x)_+ = \max\{x, 0\}$. Under the normality assumption for *E*, the expectations $\mathrm{E}[(E-T)_+]$ and $\mathrm{E}[(T-E)_+]$ have closed-form expressions involving the standard normal *pdf* and *cdf*, which are implemented in an auxiliary function ETC_single. The scalar optimization is carried out using the Matlab routine *fminbnd*, yielding the optimal Q^* and the associated marginal price $p_C^*(Q^*)$ for each firm.

Using this procedure, the program computes for all 46 firms the mean emissions μ_E, emission volatility σ_E, maximum CCER use Q_{max} and the model-implied marginal CCER prices at $Q=0, Q=Q_{max}$ and $Q=Q^*$. The numerical results show that: (1) for all firms, the predicted marginal price at zero CCER usage is identical and equals $p_C^*(0) = 72.50\ \mathrm{CNY/t}$. This is because at $Q=0$ we have $T = A = \mu_E$, so $\Phi(0) = 0.5$ and

$$p_C^*(0) = v_{res} + (\bar{p}_A - v_{res})(1 - \Phi(0)) = 30 + (115-30)\times 0.5 = 72.5. \quad (2)$$

When firms use CCER up to the policy cap $Q_{max} = \alpha\mu_E$, the marginal willingness-to-pay falls for all firms to approximately $p_C^*(Q_{max}) \approx 47.52\ \mathrm{CNY/t}$, because additional CCERs raise the total compliance position $T = A+Q$ and reduce the probability that the firm ends up short and needs to settle at the higher CEA price $\bar{p}_A$. (3) The optimization results show that for every firm in the sample, the cost-minimizing choice is $Q^* = Q_{max}$, so $p_C^*(Q^*) = p_C^*(Q_{max}) \approx 47.52\ \mathrm{CNY/t}$.

The program also computes emission-weighted average theoretical CCER prices across all firms (using μ_E as weights). The results are $(\mathrm{CNY/t})$: Mean $p_C^*(Q=0) = 72.50$, Mean $p_C^*(Q=Q_{max}) = 47.52$, Mean $p_C^*(Q=Q^*) = 47.52$.

Because all firms optimally choose $Q^* = Q_{max}$, the average optimal marginal price coincides with the marginal price at the cap. The left graph in **Figure 1** illustrates the marginal willingness-to-pay curve $p_C^*(Q)$ for a representative firm, chosen in the code as the one whose

expected emissions are closest to the sample median, namely the firm with ticker 966, for which (t CO2) $\mu_E = 657,528, \sigma_E = 40,093.29, A = 657,528, \quad Q_{max} = 32,876.40$. The horizontal axis of the left graph in **Figure 1** plots Q (in million tonnes CO2) from 0 to $Q_{\max}$, and the vertical axis reports $p_C^*(Q)$ in CNY/t. The curve starts at $p_C^*(0) = 72.50 \text{ CNY/t}$ and monotonically declines to $p_C^*(Q_{max}) \approx 47.52 \text{ CNY/t}$ as Q increases, with two horizontal reference lines at $\bar{p}_A = 115 \text{ CNY/t}$ and $v_{res} = 30 \text{CNY/t}$. The points Q=0, $Q = Q_{max}$ and $Q = Q^*$ are highlighted on the curve; since for this firm $Q^* = Q_{max} = 32,876.40 \text{ t CO2}$, the last two coincide and $p_C^*(Q^*) = p_C^*(Q_{max}) \approx 47.52 \text{ CNY/t}$. The right graph in **Figure 1** summarizes the cross-sectional distribution of $p_C^*(Q^*)$ for all 46 firms. The horizontal axis is $p_C^*(Q^*)$ (CNY/t) and the vertical axis is the number of firms. The descriptive statistics are: $\min p_C^*(Q^*) = 47.51 \text{ CNY/t}, \max p_C^*(Q^*) = 47.53 \text{ CNY/t},$ mean $= 47.52 \text{ CNY/t}$, median $= 47.52 \text{ CNY/t}$, $\text{std.dev.} \approx 0.00 \text{CNY/t},$ indicating an extremely concentrated distribution.

Overall, the numerical results yield three main conclusions. First, when firms hold allowances equal to their expected emissions, the initial marginal value of CCER at zero usage is exactly halfway between the residual CCER value and the expected CEA price, that is $p_C^*(0) = \frac{1}{2}(\bar{p}_A + v_{res}) = 72.5 \text{ CNY/t}$. Second, as firms increase CCER usage up to the regulatory cap, their marginal willingness-to-pay declines to about 47.52 CNY/t, but remains well above the residual value of 30 CNY/t, which supports a non-trivial economic value of CCER under the given market conditions. Third, under the current parameterization all firms optimally choose $Q^* = Q_{max}$, so the cross-sectional dispersion of $p_C^*(Q^*)$ is negligible, as illustrated by the right graph in **Figure 1**.

These findings highlight both the internal consistency and the limitations of the current calibration. The income-approach model delivers a transparent relationship between the CEA price, the CCER residual value and firms' optimal CCER demand, while the near-degeneracy of the cross-sectional distribution suggests that richer heterogeneity in allowance allocation rules, emission uncertainty and firm-specific constraints, or relaxing the assumption $A = \mu_E$ for all firms, would generate a wider and more realistic spread of $p_C^*(Q^*)$ than that shown in the right graph in **Figure 1**.

4. Macro-level CCER valuation: from the market's perspective

In this section, we employ the market approach to model carbon prices through a regime-switching geometric Brownian motion (GBM). Compared to a single-regime GBM, this framework is capable of capturing structural shifts in economic activity, energy demand, and regulatory policies, thereby depicting the nonlinear, state-dependent dynamics of CEA and CCER. We treat CEA prices as the underlying asset in a risk-neutral regime-switching GBM and value CCER as a real option, while considering observable price boundaries, offset substitutability with CEA, and policy-mandated offset ratio constraints.

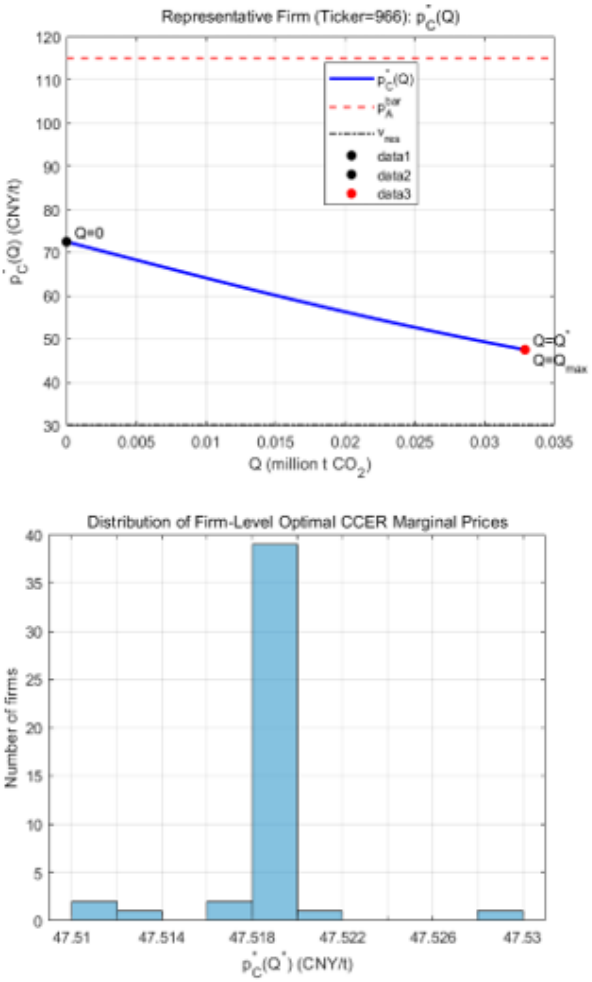

Figure 1. Representative-firm marginal CCER pricing curve and cross-sectional distribution of optimal marginal CCER prices

4.1. Theoretical analysis of the value-relevance of CCER and CEA

For compliance enterprises, one unit of CCER can either offset one ton of verified emissions on the compliance date or be sold on the secondary market before its expiration, thus representing a flexible right. Holding CCER units with an expiration date of T at time zero grants the holder the right to choose between compliance use and market sale, with the higher benefit prevailing at or before time T. Let P_t^A and P_t^C be CEA and CCER prices at time t, and r the continuously compounded risk-free rate. Empirically P_t^C is usually below P_t^A and bounded below by a residual value v_{res}, so a basic restriction is $0 \le v_{res} \le P_t^C \le P_t^A$.

We approximate the marginal compliance value of one CCER at T by an increasing function $f(P_T^A)$ of the settlement CEA price. Under full subtitutability and ignoring firm-specific constraints, we use

$f\left(P_T^A\right)=\min\left\{P_T^A,\bar{p}_{\boldsymbol{A}}{}^{max}\right\}$, where $\bar{p}_{\boldsymbol{A}}{}^{max}$ is an effective cap on the CEA settlement price. The time-zoo CCER value under the risk-neutral measure Q is $V_0^C=e^{-rT}\mathrm{E}^{\mathrm{Q}}\left[f\left(P_T^A\right)\right]$, which is constrained to satisfy $v_{res}\le V_0^C\le V_0^A$, where V_0^A is the risk-neutral value of one CEA unit. Calibration of f(·) is chosen so that the implied ratio $\theta_t=P_t^C/P_t^A$ lies in the empirical band $\underline{\theta}\le\theta_t\le\bar{\theta}$.

In the Beijing CCER market, **Table 1** indicates that θ_t is typically between 0.56 and 1.08, with $P_t^C\le P_t^A$ and a common range around 0.6 to 0.7. To reflect this structure, we specify a state-dependent pricing kernel $P_t^C=\theta(\alpha_t)P_t^A$, where α_t is an unobserved economic regime and $\theta(\alpha_t)$ is the CCER-CEA price ratio in regime α_t. Given the regime-switching process for P_t^A, CCER prices are thus driven jointly by P_t^A and the regime index α_t.

Regime uncertainty is modeled by a continuous-time finite-state Markov chain $(\alpha_t)_{t\ge0}$ with state space $\mathrm{M}=\{e_1,e_2,\ldots,e_m\}$, representing different macro or regulatory conditions. For more details of Markov chain's modelling and applications, we refer to (Zheng *et al.*, 2020; Ni *et al.*, 2024; Xu *et al.*, 2024). The "regime" can be understood as a combination of high, medium, and low levels of temperature and industrial activity, or more broadly as a state defined by temperature, coal prices, industrial added value growth rates, and regulatory policy dynamics. This Markov chain determines the drift rate, volatility, and spread ratio θ(·) of the CEA price process, and therefore transmits regime shifts into CCER valuation.

4.2. Modeling CEA and CCER prices with regime-switching geometric Brownian motion

We now specify a regime-switching geometric Brownian motion (GBM) for CEA and CCER prices. Let $(B_t)_{t\ge0}$ be a standard Brownian motion and $(\alpha_t)_{t\ge0}$ a continuous-time Markov chain on $\mathrm{M}=\{e_1,\ldots,e_m\}$ with generator $Q=\left(q_{ij}\right)_{1\le i,j\le m}$, where $q_{ij}\ge0$ for i≠j and $q_{ii}=-\sum_{j\ne i}q_{ij}$. The filtered probability space is $\left(\Omega,\mathrm{F},(\mathrm{F}_t)_{t\ge0},\mathrm{P}\right)$, with filtration generated by B_t and α_t. Under P, the CEA price $\left(P_t^A\right)_{t\ge0}$ follows

$$\mathrm{d}P_t^A=\mu_A(\alpha_t)P_t^A\mathrm{d}t+\sigma_A(\alpha_t)P_t^A\mathrm{d}B_t,0\le t\le T, \tag{4.1}$$

with regime-specific drift $\mu_A(i)$ and volatility $\sigma_A(i)>0$. The solution is $P_T^A=P_0^A\exp\left(\int_0^T\left(\mu_A(\alpha_u)-\frac{1}{2}\sigma_A^2(\alpha_u)\right)du+\int_0^T\sigma_A(\alpha_u)dB_u\right)$.

To price under no arbitrage, we move to a risk-neutral measure Q such that $e^{-rt}P_t^A$ is a martingale. Let $\lambda_t=\left(\mu_A(\alpha_t)-r\right)/\sigma_A(\alpha_t)$ and define $\frac{\mathrm{dQ}}{\mathrm{dP}}=\exp\left(-\int_0^T\lambda_u dB_u-\frac{1}{2}\int_0^T\lambda_u^2du\right)$. Then $\tilde{B}_t=B_t+\int_0^t\lambda_u du$ is a Q-Brownian motion and

$$dP_t^A=rP_t^Adt+\sigma_A(\alpha_t)P_t^Ad\tilde{B}_t, \tag{4.2}$$

or equivalently $P_T^A=P_0^A\exp\left(\int_0^T\left(r-\frac{1}{2}\sigma_A^2(\alpha_u)\right)du+\int_0^T\sigma_A(\alpha_u)d\tilde{B}_u\right)$. We keep the generator *Q* unchanged under Q ,which is standard and sufficient for pricing here.

To link CEA and CCER prices by regime, we introduce $\theta(i)\in\left[\underline{\theta},\bar{\theta}\right],i=1,\ldots,m,$ calibrated from CCER/CEA price ratios. When $\alpha_t=e_i$, we set

$$P_t^C=\theta(\alpha_t)P_t^A, \tag{4.3}$$

so that in regime *i* the CCER price is a fixed fraction θ(*i*) of the CEA price. Combining (4.2) and (4.3) and using Ito's formula, for fixed regime *i* we obtain

$$\mathrm{d}P_t^C=\theta(i)\mathrm{d}P_t^A=rP_t^C\mathrm{d}t+\sigma_C(i)P_t^C\mathrm{d}\tilde{B}_t,\sigma_C(i)=\sigma_A(i),$$

so $\left(P_t^C\right)_{t\ge0}$ also follows a regime-switching GBM under Q: $\mathrm{d}P_t^C=rP_t^C\mathrm{d}t+\sigma_C(\alpha_t)P_t^C\mathrm{d}\tilde{B}_t$.

For valuation, let g(·) be the marginal compliance value of one CCER at maturity *T* as a function of P_T^A. A simple specification with full substitutability and a floor is $g\left(P_T^A\right)=\max\left\{v_{\mathrm{res}},\theta_{\mathrm{eff}}P_T^A\right\}$ with $\theta_{\mathrm{eff}}\in\left[\underline{\theta},\bar{\theta}\right]$. The time-zero value of a CCER unit is

$$V_0^C=e^{-rT}\mathrm{E}^{\mathrm{Q}}\left[g\left(P_T^A\right)\mid P_0^A=p_0^A,\alpha_0=e_i\right], \tag{4.4}$$

where P_0^A is the current CEA price and e_i the current regime. Due to regime switches, P_T^A is not lognormal and (4.4) has in general no closed form. Two standard numerical approaches are therefore used: a system of coupled PDEs, or Monte Carlo simulation (see Hu *et al.*, 2020; Liang *et al.*, 2022 for more applications).

For the PDE approach, define $v_i(p,t)$ as the value at time t of one CCER when $P_t^A=p$ and $\alpha_t=e_i,i=1,\ldots,m.$ Then $v=(v_1,\ldots,v_m)$ solves, on $(p,t)\in(0,\infty)\times[0,T)$

$$\frac{\partial v_i}{\partial t}+\frac{1}{2}\sigma_A^2(i)p^2\frac{\partial^2v_i}{\partial p^2}+rp\frac{\partial v_i}{\partial p}-rv_i+\sum_{j=1}^m q_{ij}v_j=0 \tag{4.5}$$

with terminal condition $v_i(p,T)=g(p).$ Numerical schemes such as finite differences can be used to obtain $v_i\left(p_0^A,0\right)$, so that $V_0^C=v_i\left(p_0^A,0\right)$. For Monte Carlo,one simulates *N* paths of $\left(P_t^A,\alpha_t\right)$ under Q on [0,*T*] using (4.2) and the Markov chain with generator *Q*. For each path *k*, record

$P_T^{A,(k)}$ and compute $g\left(P_T^{A,(k)}\right)$; then $\hat{V}_0^C = e^{-rT}\frac{1}{N}\sum_{k=1}^{N} g\left(P_T^{A,(k)}\right)$, which converges to V_0^C as $N \to \infty$. Alternatively, one may simulate P_t^C directly via (4.3) and use a payoff $h\left(P_T^C\right)$, for instance $h\left(P_T^C\right) = \max\left\{P_T^C - K_C, v_{res}\right\}$ with a strike K_C and then compute $\tilde{V}_0^C = e^{-rT}\mathrm{E}^{\mathrm{Q}}\left[h\left(P_T^C\right)\right]$. With suitable choices of g and *h* consistent with (4.3), the two formulations are equivalent.

Calibration proceeds in two steps. First, regimes are identified from exogenous variables such as daily temperature and industrial added value growth, for example by partitioning the (x,y)-plane with $y = x + c_1$ and $y = x + c_2$ and assigning each day to a regime.The transition rates q_{ij} are then estimated from empirical holding times and transition counts. Second, given regime labels, regime-specific drifts $\mu_A(i)$ and volatilities $\sigma_A(i)$ are estimated from CEA log returns, and the spread parameters $\theta(i)$ from paired CEA-CCER prices,subject to $\underline{\theta} \le \theta(i) \le \bar{\theta}$. Once $\{Q, \mu_A(i), \sigma_A(i), \theta(i)\}_{i=1}^{m}$ and r are calibrated, the regime-switching GBM fully specifies the joint dynamics of CEA and CCER prices under Q, and thus yields a CCER value V_0^C that reflects regime uncertainty, empirical spreads and the real options nature of CCER.

4.3. Numerical implementation and discussion on the results

This subsection uses the Matlab code (refer to Appendix C) to implement a three-regime Markov switching GBM for CEA and CCER and to price a guarantee-type payoff $E\left[\max\left(CCER_T, K\right)\right]$ under the risk-neutral measure. Daily 2023 CEA and CCER prices from Beijing Green Exchange are combined with monthly year-on-year electricity growth. The monthly growth rates are mapped to the daily grid; empirical quantiles of both electricity growth and CEA price define three regimes: regime 1 (low growth, low price), regime 3 (high growth, high price), and regime 2 (intermediate). If any regime is too small, its days are merged into the middle regime.

Within each regime $s \in \{1,2,3\}$, the drift and volatility of daily CEA log returns are estimated as sample mean and standard deviation, giving $\mu_A(s)$ and $\sigma_A(s)$. The Markov transition matrix *P* is built from observed one-step regime switches. For CCER, an equilibrium relation $S_t^C \approx \theta_s S_t^A$ is assumed, where θ_s is the average CCER/CEA ratio in regime s, truncated to [0.5,1.0]. In simulation, $S_t^C = \theta_s S_t^A$ times an idiosyncratic lognormal shock (Rasool *et al.*, 2020; Shabbir *et al.*, 2020; Zhang *et al.*, 2020; Hussain *et al.*, 2021; Yan *et al.*, 2022). The daily standard deviation of this CCER-specific noise is set at $0.10\sqrt{\Delta t}$ with $Z_t \sim N(0,1)$, which generates realistic short-run deviations between CCER and CEA while preserving long-run co-movement through θ_s.

Under the risk-neutral measure, CEA in regime s follows a GBM with drift $r - \frac{1}{2}\sigma_s^2$ and volatility σ_s, with annual risk-free rate r=0.0435 and time step Δt=1/252. At each step, the regime is updated using P, then CEA is evolved by the corresponding GBM, and CCER is obtained as $\theta_s S_t^A$ times the idiosyncratic shock. The code simulates joint paths of CEA and CCER over T_{trade}=80 trading days from end-2023 levels, with initial prices $S_0^A = 111.38\ \mathrm{CNY}$ and $S_0^C = 72.00\ \mathrm{CNY}$. The initial regime is the observed last-day regime. The guarantee level is $K = 72.00\ \mathrm{CNY}$.

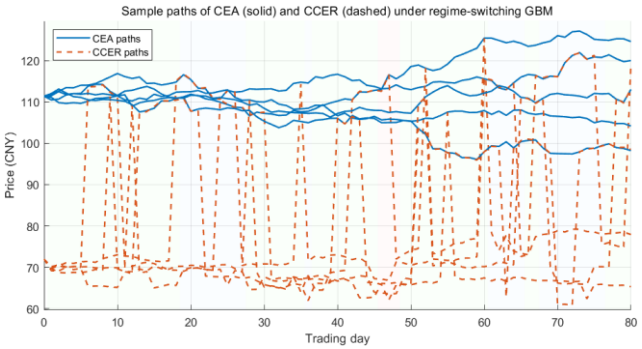

Figure 2. Simulated CEA (solid) and CCER (dashed) price paths over 80 trading days under a three-regime switching GBM, with background color bands indicating low, medium, and high demand-price regimes

Figure 2 illustrates five simulated paths over 80 days. Solid lines are CEA, dashed lines CCER. The background bands show the simulated regimes: blue for regime 1, green for regime 2, red for regime 3. Regimes evolve endogenously according to P. CEA and CCER co-move at the regime scale, with higher growth of both prices and higher volatility in red bands, and flatter or downward behavior in blue bands. Regime-specific $\sigma_A(s)$ generates time-varying volatility. The larger CCER idiosyncratic noise $0.10\sqrt{\Delta t}$ produces visible but transient deviations of CCER from $\theta_s S_t^A$, consistent with CCER's lower liquidity and project heterogeneity. The paths combine long-run co-movement, regime-dependent risk and short-run spread fluctuations.

On this joint dynamics, the value of a single-maturity payoff $\max\left(CCER_T, K\right)$ with $\mathrm{T} = 80$ days is approximated by Monte Carlo: $\mathrm{PV} = e^{-rT}\mathrm{E}^{\mathrm{Q}}\left[\max\left(CCER_T, K\right)\right]$ with 20,000 paths. The output is $\mathrm{PV} \approx 80.4027\ \mathrm{CNY}$ per unit CCER, compared with spot $S_0^C = 72.00\ \mathrm{CNY}$ and $K = 72.00\ \mathrm{CNY}$. Since $\max\left(CCER_T, K\right)$ equals one CCER plus a European call with strike *K*, the excess $\mathrm{PV} - S_0^C \approx 8.4\ \mathrm{CNY}$ reflects option value from regime-driven upside and the floor at *K*.

To illustrate how the guarantee value varies with initial CEA S_0^A and maturity *T*, a grid is set with S_0^A from 80.00

to 160.00 CNY (25 points) and *T* from 10 to 80 trading days (step 10). At each grid point $\left(S_0^A, T\right)$, 15,000 paths of the joint process are simulated, the payoff $\max\left(CCER_T, K_2\right)$ is computed and discounted. The guarantee level is $K_2 = K_{base} + \alpha_{\text{follow}}\theta_{\text{mid}}\left(S_0^A - S_0^{\text{CEA}}\right)$, where $K_{base} = 72.00\ \text{CNY}, \theta_{mid} = 0.6257$ is the middle-regime ratio, $S_0^{\text{CEA}} = 111.38\ \text{CNY}$ is the current CEA price, and $\alpha_{\text{follow}} = 0.30$. Thus only 30 percent of deviations of S_0^A from S_0^{CEA} feed into the floor, which weakens the almost linear dependence that would occur under $K_2 = \theta_{\text{mid}} S_0^A$.

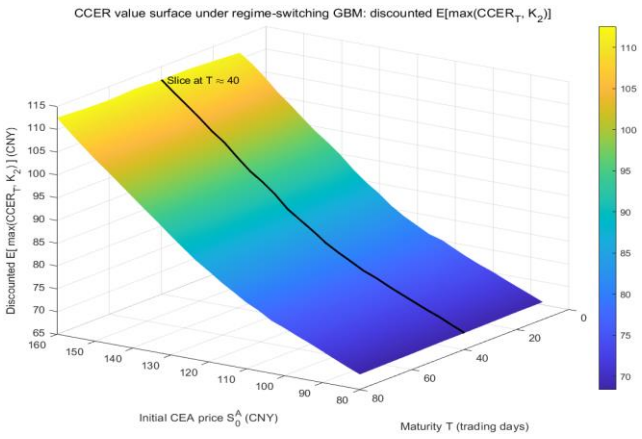

Figure 3. Discounted expected value surface $E\left[\max\left(CCER_T, K_2\right)\right]$ per unit CCER under the regime-switching GBM, as a function of initial CEA price and maturity, with the guarantee level defined as a baseline plus a partially adjusting component

Figure 3 reports the discounted expectation $\text{EQ}\left[\max\left(CCER_T, K_2\right)\right]e^{-rT}$ on this grid (with simple interpolation). Along the *T* direction, holding S_0^A fixed, values increase with maturity because the process has more chances to enter high-demand regimes and the time value of the floor-contract outweighs discounting. Along S_0^A, each maturity slice is upward-sloping but nonlinear: with $K_2 = K_{base} + 0.30\ \theta_{\text{mid}}\left(S_0^A - S_0^{\text{CEA}}\right)$, the floor adjusts slower than the expected terminal CCER level as S_0^A rises, so the marginal impact of S_0^A gradually declines at high initial prices. In the low S_0^A region, values remain clearly above k_{base} even at short horizons, indicating a nontrivial probability of regime-driven recovery before maturity. A slice at $\text{T} \approx 40$ days (black curve) highlights this nonlineaeity: near S_0^{CEA} the slope in S_0^A is steep, then flattens at higher S_0^A ,confirming the dampened pass-through of initial price into guarantee value under the partial-follow rule.

5. Comparison and summary

5.1. Comparing micro-level and macro-level CCER valuation results

This subsection compares the micro-benefit approach in Section 3 with the macro-regime switching GBM approach in Section 4. By examining the implied marginal or fair CCER price (unit: yuan/ton) of the model and aligning key calibration items (such as expected CEA settlement prices, CCER residual values, and observed CEA and CCER spot prices), the two methods are made comparable.

On the micro side, Section 3 studies a representative compliance enterprise minimizing expected total compliance cost under uncertain emissions, regulatory caps and residual value risk. The firm faces random annual emissions *E* with mean μ_E and variance σ_E^2, allowance allocation *A*, maximum CCER usage $Q_{\max} = \alpha\mu_E$, expected marginal CEA settlement price $\bar{p}_A$, and residual value v_{res}. Total cost equals upfront CCER spending plus expected CEA gap-filling cost minus expected residual liquidation value. Treating $Q \in \left[0, Q_{max}\right]$ as continuous, the first-order condition yields a marginal willingness-to-pay $p_C^{\varepsilon}(Q) = v_{\text{res}} + \left(\bar{p}_A - v_{\text{res}}\right)\left[1 - \Phi\left(\left(A + Q - \mu_E\right)/\sigma_E\right)\right]$, interpreted as a weighted average of $\bar{p}_A$ and v_{res}, with the weight on $\bar{p}_A$ given by the emission shortfall probability after purchasing Q.

Under the baseline calibration with offset ratio $\alpha = 0.05, \bar{p}_A = 115\ \text{CNY/t}$, $v_{res} = 30\ \text{CNY/t}$, allocation $A = \mu_E$, and approximately normal emissions, the model is applied to 46 low- and normal-emission firms. For each, μ_E, σ_E, Q_{max} and $p_C^{\varepsilon}(0)$, $p_C^{\varepsilon}(Q_{max}), p_C^{\varepsilon}\left(Q^{\varepsilon}\right)$ are computed. All firms obtain $Q^{\varepsilon} = Q_{max}$, that is optimal usage at the cap.At $\text{Q} = 0$, the shortfall probability equals 1/2 so $p_C^{\varepsilon}(0) = \frac{1}{2}\left(\bar{p}_A + v_{res}\right) = 72.50\ \text{CNY/t}$. At Q*max* the shortfall probability is much lower and the marginal value drops to about $47.52\ \text{CNY/t}$. The emission-weighted distribution of $p_C^{\varepsilon}\left(Q^{\varepsilon}\right)$ is thus very concentrated around $47.52\ \text{CNY/t}$.

On the macro side, Section 4 models CEA and CCER via a three-regime switching GBM calibrated to 2023 Beijing data and electricity growth, with regimes capturing low, medium and high demand-price environments through a finite-state Markov chain. Within each regime, CEA follows a risk-neutral GBM; CCER equals a regime-dependent fraction of CEA times an idiosyncratic lognormal shock with daily standard deviation $0.10\sqrt{\Delta t}$, representing CCER-specific noise. CCER is then valued as a real-option-like asset whose payoff reflects its compliance substitutability and residual value.

For a single-maturity payoff $\max\left(CCER_T, K\right)$ with $\text{T} = 80$ days, $\text{K} = 72$ CNY, r=0.0435, and starting prices $S_0^A = 111.38\ \text{CNY}$, $S_0^C = 72.00\ \text{CNY}$, Monte Carlo with 20000 paths gives $\text{PV} \approx 80.40\ \text{CNY/t}$. The excess over spot is the value of the embedded call on CCER under regime uncertainty. Extending to a grid over S_0^A and T with a guarantee K_2 anchored at 72 CNY and partially following S_0^A yields a surface $\text{E}^{\text{Q}}\left[\max\left(CCER_T, K_2\right)\right]e^{-rT}$ that increases

with T and displays nonlinear dependence on S_0^A . As follows, **Table 1** summarizes representative outcomes.

Table 1. Comparison between micro-level and macro-level CCER valuation results

	Micro-level income approach (firm perspective)	**Macro-level market approach (regime-switching GBM)**
Modeling focus	representative firm or firm sample	Risk-neutral pricing of CCER as a real option-like asset under state-dependent price dynamics
Main uncertainty source	Firm-level emission risk (μ_E, σ_E) with prices and residual value exogenous	Stochastic CEA and CCER prices driven by a three-regime switching GBM
Decision variable or contract type	CCER purchase quantity $Q \in [0, Q_{\max}]$ chosen once per period	Holding CCER and possibly a guarantee-type contract max($CCER_T$, K) or max($CCER_T$, K_2)
Representative price	$p_C^{\varepsilon}(0) = 72.50$;	PV≈80.40 at T=80 days
levels (CNY/t)	$p_C^{\varepsilon}(Q_{\max}) \approx 47.52$; $p_C^{\varepsilon}(Q^{\varepsilon}) \approx 47.52$	and K=72; CCER spot at t=0:72.00
Treatment of residual or floor value	Constant residual value ν_{res} at period end	Floor K or K_2 at maturity under regime uncertainty
Time structure	One-period static compliance decision	Multi-period stochastic evolution over up to 80 trading days

The micro model produces CCER values between ν_{res} and $\bar{p}_A$, with precise levels driven by shortfall probabilities. Under the condition of homogeneous parameters and A=μ_E, the marginal value converges around 47.52 CNY/t at the upper limit and is 72.50 CNY/t at zero usage, which can serve as a conservative benchmark from a static performance perspective. When applied to contracts with clear lower limits, macro models typically yield higher valuations as they price the upside potential and time value of flexibility in favorable regimes; the guaranteed rights with an exercise price of K=72 CNY reach approximately 80.40 CNY/t, which is higher than the spot price and the micro-level marginal value.

This difference reflects different economic roles. In the micro-scenario, CCER hedges the specific emission risks of enterprises within a single compliance cycle; once the enterprise comfortably meets the compliance requirements, the valuation of additional CCER approaches ν_{res}. In the macro-scenario, CCER is a tradable asset exposed to macro-regime shifts, with valuation using the complete risk-neutral distribution of future prices, and the right-tail state is amplified due to the lower bound. Therefore, earnings-based valuation is suitable for internal compliance analysis and conservative reference pricing, while regime-switching GBM is more suitable for pricing structured CCER products and evaluating the risk-return characteristics of CCER positions.

5.2. Summary and future research

This article constructs a comprehensive CCER valuation framework that combines the micro-level income approach with the macro-level regime-switching GBM, linking compliance behavior with market price dynamics.

At the micro level, a representative enterprise with uncertain emissions, fixed allowances and a binding CCER cap chooses CCER purchase quantity Q to minimize expected total compliance cost, decomposed into CCER expenditure, contingent CEA gap-filling cost and residual value of surplus assets. Under a continuous emission distribution, an explicit marginal willingness-to-pay $p_C^{\varepsilon}(Q)$ is derived as a convex combination of expected CEA price and residual value, with weights given by shortfall probabilities. Calibration to firm data under a baseline with $A=\mu_E$ and homogeneous parameters show optimal use at the cap and marginal values clustering near $47.52\ \text{CNY/t}$, with $p_C^{\varepsilon}(0) = 72.50\ \text{CNY/t.}$

At the macro level, CEA and CCER follow a three-regime switching GBM calibrated to 2023 Beijing data and electricity growth. Regimes imply state-dependent drift- s and volatilities; CCER is a regime-dependent fraction of CEA with idiosyncratic noise. CCER is valued as a real-option-like asset. For $\max(CCER_T, K)$ with $\mathrm{T} = 80$ days and K equal to spot, Monte Carlo yields about $80.40\ \text{CNY/t}$, above spot and micro-level marginal values. A grid over initial CEA prices and maturities with K_2 defined as a baseline plus partial adjustment generates a value surface that increases with T and responds nonlinearly to S_0^A , highlighting the interaction between regimes, price risk and contract design.

The two layers achieve the following objectives together: (1) they connect firm-specific emission risk and regulatory parameters to CCER valuations and optimal purchase quantities; (2) they embed CCER pricing within a regime-sensitive risk-neutral framework that captures empirical features including regime-dependent volatility and CEA-CCER spreads; (3) they demonstrate how guarantee-type structures alter CCER value and link compliance instruments with CCER-based financial products.

Future research could relax the micro-model assumptions on allocation, offset ratios and residual values to accommodate richer heterogeneity, and expand the macro model by incorporating time-varying transition

intensities, jump processes or stochastic volatility, alongside a more granular CEA-CCER spread process. A particularly promising direction involves tighter coupling of the two layers, where macro price dynamics generate endogenous inputs for the micro model while firm-level CCER demand feeds back into the market model, thereby enabling analysis of the feedback mechanisms among compliance behavior, policy design and price formation in support of carbon peaking and neutrality objectives.

References

Adade, S.Y.S.S., Lin, H., Johnson, N.A.N., *et al.* Advanced food contaminant detection through multi-source data fusion: Strategies, applications, and future perspectives[J]. Trends in Food Science & Technology, 2025, 156.

Alessi, L., Ossola, E., Panzica, R. When do investors go green? Evidence from a time-varying asset-pricing model[J]. International Review of Financial Analysis, 2023, 90: 102898.

Barker, R., Lennard, A., Penman, S., *et al.* Accounting for intangible assets: suggested solutions[J]. Accounting and Business Research, 2022, 52(6): 601-630.

Bolton, P., Kacperczyk, M. Are carbon emissions associated with stock returns? Comment[J]. Review of Finance, 2024, 28(1): 107-109.

Chen, M., Lai, E. Carbon Asset Management System and Trading Strategies: Empowering Listed Companies in Value Reassessment and Sustainable Development[J]. Advances in Management and Intelligent Technologies, 2025, 1(6).

Chevallier, J., Goutte, S., Ji, Q., *et al.* Green finance and the restructuring of the oil-gas-coal business model under carbon asset stranding constraints[J]. Energy Policy, 2021, 149: 112055.

Dong, X., Yoon, S.M. Effect of weather and environmental attentions on financial system risks: Evidence from Chinese high- and low-carbon assets[J]. Energy Economics, 2023, 121: 106680.

Dutta, A., Dutta, P. Geopolitical risk and renewable energy asset prices: Implications for sustainable development[J]. Renewable Energy, 2022, 196: 518-525.

Green, J.F. Does carbon pricing reduce emissions? A review of ex-post analyses[J]. Environmental Research Letters, 2021, 16(4): 043004.

Hao, J., Deng, Z., Li, J., *et al.* How to price a dataset: a deep learning framework for data monetization with alternative data[J]. Humanities and Social Sciences Communications, 2025, 12: 1736.

Hu, D., Sun, T., Yao, L., *et al.* Monte Carlo: A flexible and accurate technique for modeling light transport in food and agricultural products[J]. Trends in Food Science & Technology, 2020, 102: 280-290.

Hussain, S., Hussain, S., Aslam, Z., *et al.* Impact of Different Water Management Regimes on the Growth, Productivity, and Resource Use Efficiency of Dry Direct Seeded Rice in Central Punjab-Pakistan[J]. Agronomy-Basel, 2021, 11(6).

Jeny, A., Moldovan, R. Accounting for intangible assets - insights from meta-analysis of R&D research[J]. Journal of Accounting Literature, 2022, 44(1): 40-71.

Langley, P., Bridge, G., Bulkeley, H., *et al.* Decarbonizing capital: Investment, divestment and the qualification of carbon assets[J]. Economy and Society, 2021, 50(3): 494-516.

Li, W., Zhang, C., Ma, T., *et al.* Estimation of summer maize biomass based on a crop growth model[J]. Emirates Journal of Food and Agriculture, 2021, 33(9): 742-750.

Liang, Z., Li, J., Liang, J., *et al.* Investigation into Experimental and DEM Simulation of Guide Blade Optimum Arrangement in Multi-Rotor Combine Harvesters[J]. Agriculture-Basel, 2022, 12(3).

Liu, Y., Tian, L., Sun, H., *et al.* Option pricing of carbon asset and its application in digital decision-making of carbon asset[J]. Applied Energy, 2022, 310: 118375.

Liu, Y., Tian, L., Xie, Z., *et al.* Option to survive or surrender: Carbon asset management and optimization in thermal power enterprises from China[J]. Journal of Cleaner Production, 2021, 314: 128006.

Liu, Y., Lu, X., Sun, H.P., *et al.* Optimization of carbon performance evaluation and its application to strategy decision for investment of green technology innovation[J]. Journal of Environmental Management, 2023, 325A: 116593.

Liu, Y., Sun, H.P., Meng, B., *et al.* How to purchase carbon emission right optimally for energy-consuming enterprises? Analysis based on optimal stopping model[J]. Energy Economics, 2023, 124: 106758.

Mahmood, F., Ali, M., Khan, M., *et al.* A review of biochar production and its employment in synthesizing carbon-based materials for supercapacitors[J]. Industrial Crops and Products, 2025, 227.

Mengesha, I., Roy, D. Carbon pricing drives critical transition to green growth[J]. Nature Communications, 2025, 16: 1321.

Nazir, M.J., Li, G., Nazir, M.M., *et al.* Harnessing soil carbon sequestration to address climate change challenges in agriculture[J]. Soil & Tillage Research, 2023, 237.

Ni, J., Xue, Y., Zhou, Y., *et al.* Rapid identification of greenhouse tomato senescent leaves based on the sucrose-spectral quantitative prediction model[J]. Biosystems Engineering, 2024, 238: 200-211.

Ni, J., Xue, Y., Zhou, Y., *et al.* Rapid identification of greenhouse tomato senescnt leaves based on the sucrose-spectral quantitative prediction mode[J]. Biosystems Engineering, 2024, 238: 200-211.

Pechlivanidis, E., Ginoglou, D., Barmpoutis, P. Can intangible assets predict future performance? A deep learning approach[J]. International Journal of Accounting & Information Management, 2022, 30(1): 61-72.

Rasool, G., Guo, X., Wang, Z., *et al.* Coupling fertigation and buried straw layer improves fertilizer use efficiency, fruit yield, and quality of greenhouse tomato[J]. Agricultural Water Management, 2020, 239.

Raza, S., Irshad, A., Margenot, A., *et al.* Inorganic carbon is overlooked in global soil carbon research: A bibliometric analysis[J]. Geoderma, 2024, 443.

Sadalage, P.S., Dar, M.A., Bhor, R.D., *et al.* Optimization of biogenic synthesis of biocompatible platinum nanoparticles with catalytic, enzyme mimetic and antioxidant activities[J]. Food Bioscience, 2022, 50.

Shabbir, A., Mao, H., Ullah, I., *et al.* Effects of Drip Irrigation Emitter Density with Various Irrigation Levels on Physiological Parameters, Root, Yield, and Quality of Cherry Tomato[J]. Agronomy-Basel, 2020, 10(11).

hao, L., Gong, J., Fan, W., *et al.* Cost Comparison between Digital Management and Traditional Management of Cotton Fields-

Evidence from Cotton Fields in Xinjiang, China[J]. Agriculture-Basel, 2022, 12(8).

Siddique, M.A., Nobanee, H., Hasan, M.B., *et al.* How do energy markets react to climate policy uncertainty? Fossil vs. renewable and low-carbon energy assets[J]. Energy Economics, 2023, 128: 107195.

Su, C.W., Pang, L.D., Qin, M., *et al.* The spillover effects among fossil fuel, renewables and carbon markets: Evidence under the dual dilemma of climate change and energy crises[J]. Energy, 2023, 274: 127304.

Van Benthem, A.A., Crooks, E., Giglio, S., *et al.* The effect of climate risks on the interactions between financial markets and energy companies[J]. Nature Energy, 2022, 7: 690-697.

Van Criekingen, K., Bloch, C., Eklund, C. Measuring intangible assets - A review of the state of the art[J]. Journal of Economic Surveys, 2022, 36(5): 1539-1558.

Van den Bremer, T.S., Van der Ploeg, F. The risk-adjusted carbon price[J]. American Economic Review, 2021, 111(9): 2782-2810.

von Dulong, A. Concentration of asset owners exposed to power sector stranded assets may trigger climate policy resistance[J]. Nature Communications, 2023, 14: 6442.

Wang, H., Liu, J., Zhang, L. Carbon emissions and assets pricing - evidence from Chinese listed firms[J]. China Journal of Economics, 2022, 9(2): 28-75.

Wang, H., Kang, Z., Yu, S., *et al.* Feasibility analysis of developing methane reduction methodologies in the oil and gas sector under the ccer reboot context[J]. Energy Storage Science and Technology, 2025, 14(4): 1709.

Wang, X., Li, J., Ren, X. Asymmetric causality of economic policy uncertainty and oil volatility index on time-varying nexus of the clean energy, carbon and green bond[J]. International Review of Financial Analysis, 2022, 83: 102306.

Xu, H., Yin, H., Liu, Y., *et al.* Regional Winter Wheat Yield Prediction and Variable Importance Analysis Based on Multisource Environmental Data[J]. Agronomy-Basel, 2024, 14(8).

Xu, H., Yin, H., Liu, Y., *et al.* Regional Winter Wheat Yield Prediction and Variable Importance Analysis Based on Multisource Environmental Data[J]. Agronomy-Basel, 2024, 14(8).

Yan, H., Ma, J., Zhang, J., *et al.* Effects of film mulching on the physiological and morphological parameters and yield of cucumber under insufficient drip irrigation[J]. Irrigation And Drainage, 2022, 71(4): 897-911.

Yang, P., Yang, L. Asset pricing and nominal price illusion in China[J]. Humanities and Social Sciences Communications, 2022, 9: 118.

Zhang, C., Li, X., Yan, H., *et al.* Effects of irrigation quantity and biochar on soil physical properties, growth characteristics, yield and quality of greenhouse tomato[J]. Agricultural Water Management, 2020, 241.

Zhang, J. Corporate carbon emissions and market value[J]. Scientific Reports, 2025, 15: 30593.

Zhang, L., Song, X., Niu, Y., *et al.* Estimating Winter Wheat Plant Nitrogen Content by Combining Spectral and Texture Features Based on a Low-Cost UAV RGB System throughout the Growing Season[J]. Agriculture-Basel, 2024, 14(3).

Zhang, S., Xue, X., Chen, C., *et al.* Development of a low-cost quadrotor UAV based on ADRC for agricultural remote sensing[J]. International Journal Of Agricultural And Biological Engineering, 2019, 12(4): 82-87.

Zhang, Z., Li, J., Guan, D. Value chain carbon footprints of Chinese listed companies[J]. Nature Communications, 2023, 14: 2794.

Appendix A

Table 2. Annual carbon emission data for low-emission enterprises (tons).

Ticker symbol	m_{i1}	m_{i2}	m_{i3}	Ticker symbol	m_{i1}	m_{i2}	m_{i3}
603388	5969	5427	4884	603778	5469	4972	4475
002431	14559	13236	11912	300008	27852	25320	22788
300536	20967	19061	17155	600072	26117	23743	21368
000037	7867	7152	6437	603717	20927	19025	17122
000993	8405	7641	6876	000711	18504	16822	15140

Source: CSMAR Database

Table 3. Annual carbon emission data for normal-emission enterprises (tons).

Ticker symbol	m_{j1}	m_{j2}	m_{j3}	Ticker symbol	m_{j1}	m_{j2}	m_{j3}	Ticker symbol	m_{j1}	m_{j2}	m_{j3}
600011	9076451	8251319	7426187	600025	839682	763347	687012	603828	109891	99901	89911
600795	3927170	3570155	3213139	000959	6749599	6135999	5522399	002542	530198	481998	433799
601991	5552259	5047508	4542757	000761	4723905	4294459	3865013	002564	716273	651157	586042
600027	6756622	6142383	5528145	600126	1990390	1809445	1628501	002628	138814	126195	113575
600023	3795945	3450859	3105773	000778	196041	178219	160397	002663	68298	62089	55880
000539	2368211	2152919	1937627	600307	1431482	1301347	1171213	002761	10519590	9563263	8606937
60002	1540961	1400873	1260786	60078	4447745	4043405	3639064	00277	72117	65561	59005

1				2				5			
000027	2276119	2069199	1862279	000709	3706154	3369231	3032308	002140	498744	453404	408063
002608	2132345	1938495	1744646	600569	2818325	2562113	2305902	300055	65169	59245	53320
600578	1708917	1553561	1398205	600282	4746223	4314748	3883274	300237	52063	47330	42597
600575	1445654	1314231	1182808	601005	1693446	1539496	1385546	300517	95146	86496	77847
600157	1533348	1393952	1254557	000825	3723184	3384713	3046241	000862	62357	56688	51019
000543	1126340	1023946	921551	600117	557233	506575	455918	300649	104958	95417	85875
600642	2127118	1933743	1740369	000717	2052221	1865655	1679090	300712	95242	86584	77925
600863	584866	531697	478527	600019	21523775	19567068	17610361	600039	7472533	6793212	6113891
000600	534253	485685	437116	000932	5453736	4957942	4462148	002116	500880	455345	409811
000767	1034726	940660	846594	600507	1269384	1153986	1038587	600133	799036	726396	653757
000966	723281	657528	591775	000898	5667263	5152057	4636852	600170	14171007	12882733	11594460
001896	782009	710918	639826	600010	3162971	2875428	2587885	600248	15423990	14021809	12619628
600780	425868	387153	348437	600022	4586444	4169495	3752545	600284	1135404	1032186	928967
600509	583520	530472	477425	600231	1027681	934255	840830	600463	61704	56094	50485
000690	452755	411595	370436	601003	4383901	3985365	3586828	600491	114836	104396	93956
600744	691180	628346	565511	600808	3801689	3456081	3110473	600502	5764712	5240647	4716582
000899	170012	154556	139101	600295	1641085	1491896	1342706	600512	526711	478828	430946
000531	238187	216534	194881	000655	137061	124601	112141	600606	29341384	26673985	24006587
600396	249379	226708	204037	600581	1509440	1372218	1234997	600667	1620650	1473318	1325987
002893	82005	74550	67095	000629	484185	440168	396152	600820	6238700	5671545	5104391
600969	204230	185664	167098	603878	161881	147165	132448	600846	431993	392721	353449
000791	95916	87197	78477	000923	190663	173330	155997	600853	753134	684667	616201
000601	317822	288929	260036	000708	8055406	7323096	6590786	600970	2317066	2106424	1895782
600483	885339	804853	724368	601969	47961	43601	39241	601117	7972458	7247689	6522920
000883	1542108	1401917	1261725	002110	4542493	4129539	3716585	601186	70552790	64138900	57725010
600900	1554752	1413411	1272070	002075	355375	323068	290761	601390	37510749	34100681	30690613
601985	3887484	3534076	3180668	600477	483255	439323	395391	601611	3506691	3187901	2869111
600886	1218380	1107618	996856	600496	1036042	941856	847670	601618	33385953	30350867	27315780
601669	26125183	23750167	21375150	601968	462657	420597	378537	601668	122315835	111196213	100076592
60082	158991	144538	130084	00275	377439	343127	308814	60166	2612518	2375016	2137515

1				6				9	3	7	0
600452	97359	88508	79657	200761	3740889	3400808	3060727	601789	945971	859974	773977
600995	124867	113515	102164	900936	1575137	1431943	1288748	601800	29555593	26868721	24181849
600116	1005080	913709	822338	002132	64877	58979	53081	603316	101724	92477	83229
600505	37156	33779	30401	002135	328280	298436	268593	603637	102229	92935	83642
000692	192555	175050	157545	002318	280555	255050	229545	603098	233934	212667	191400
600644	149033	135484	121936	002443	287503	261366	235229	603843	680770	618882	556994
000040	108142	98311	88480	002478	162868	148062	133255	603955	46973	42703	38432
000537	299017	271833	244650	002541	1520498	1382271	1244044	603959	92167	83788	75409
600167	98361	89419	80477	000629	484185	440168	396152	000032	1708014	1552740	1397466
600982	712794	647995	583195	000708	3270983	2973621	2676259	603929	101247	92043	82838
600236	274713	249739	224765	000709	3706154	3369231	3032308	002047	166202	151093	135983
600101	84140	76490	68841	000717	2052221	1865655	1679090	002081	449608	408735	367861
002039	36605	33277	29949	000961	9579035	8708214	7837393	002163	196604	178730	160857
600163	183816	167106	150395	600022	4586444	4169495	3752545	002325	149391	135810	122229
600674	50586	45988	41389	600894	433825	394386	354948	002375	585633	532393	479154
601619	60570	55064	49557	002743	318579	289617	260656	002482	56893	51721	46549
000875	755307	686642	617978	000928	1605125	1459205	1313284	002620	129069	117335	105602
002479	524052	476411	428770	000628	691222	628383	565545	002713	285503	259548	233594
600098	2634239	2394763	2155286	600939	3477904	3161731	2845558	002789	101022	91838	82654
002256	681601	619637	557673	000010	247465	224968	202471	002811	86688	78807	70926
002015	1129772	1027065	924359	000065	1761791	1601628	1441466	002822	645172	586520	527868
601016	232664	211513	190362	000090	2343598	2130543	1917489	002830	83769	76153	68538
600149	36910	33555	30199	000498	5430569	4936881	4443193	002856	71940	65400	58860
000722	31110	28282	25454	002307	997813	907102	816392	300117	70924	64476	58028
000591	303997	276361	248725	002051	113708	103371	93034	300621	755394	686722	618050
300335	63694	57904	52114	002060	949279	862981	776683	600193	94218	85652	77087
000155	231426	210387	189348	002061	3041286	2764805	2488325	601886	1443949	1312681	1181413
600979	85830	78027	70224	002062	940424	854931	769438	603030	131737	119761	107785

Source: CSMAR Database

Appendix B

```
% ================================================================
%  Income–Approach CCER Valuation (LaTeX-based, Word-data only)
% ================================================================
clear; clc; close all;

%% 1. Global parameters

alpha  = 0.05;     % Max CCER offset ratio
pA_bar = 115;      % Expected marginal CEA settlement price (CNY/t)
v_res  = 30;       % Residual value of CCER (CNY/t), must be < pA_bar

% Historical daily prices from Word data (for reference only, not used later)
aprice = [ ...
  138.00 110.40 90.00 72.00 59.00 51.47 61.80 74.20 74.20 74.20 ...
  89.00 74.00 106.80 86.00 102.00 115.64 138.50 111.00 92.22 73.80 75.00 ...
  88.77 106.60 125.00 149.64 144.30 131.75 134.00 124.00 100.90 121.00 ...
  130.12 139.00 127.00 127.00 121.77 142.00 121.88 127.00 120.00 130.00 ...
  127.00 130.00 132.53 122.50 133.50 128.00 128.00 123.03 124.00 127.50 ...
  119.18 123.57 123.77 121.28 123.00 130.29 121.35 115.13 125.25 124.94 ...
  124.17 127.93 125.17 121.38 117.72 126.25 123.03 116.89 105.28 120.71 ...
  118.88 118.44 121.37 124.41 113.92 119.90 115.96 119.96 113.01 109.92 ...
  118.49 109.91 108.16 121.72 116.00 103.32 100.00 110.00 109.00 110.00 ...
  114.34 95.00 85.06 102.00 107.00 115.00 116.00 112.00 111.38]';

cprice = [ ...
  95.00 95.00 95.00 109.00 88.00 80.00 90.00 90.89 47.00 78.00 ...
  80.00 80.00 56.40 90.00 80.00 82.00 80.00 80.00 80.00 80.34 80.00 75.00 ...
  80.00 80.00 86.96 80.00 80.01 84.81 88.00 65.64 80.00 69.70 81.40 80.00 ...
  69.38 70.50 80.44 83.90 78.23 86.00 86.99 80.00 80.00 74.77 77.63 74.50 ...
  75.00 80.10 85.40 80.00 74.00 70.42 78.00 79.51 79.14 85.00 80.00 75.00 ...
  65.00 65.00 74.60 65.01 70.00 90.00 70.00 72.00 72.00 72.00]';

%% 2. Firm-level emission data from Word (appendix tables)

% 2.1 Low-emission firms (Table 2)
% Columns: [Ticker, E_upper, E_mid, E_lower]
low_tab = [ ...
  603388 5969 5427 4884; ...
  2431   14559 13236 11912; ...  % keep numeric consistency for leading zero tickers
  300536 20967 19061 17155; ...
  37     7867 7152 6437; ...
  993    8405 7641 6876; ...
  603778 5469 4972 4475; ...
  300008 27852 25320 22788; ...
```

```
 600072 26117 23743 21368; ...
 603717 20927 19025 17122; ...
 711    18504 16822 15140];

ticker_low = low_tab(:,1);
E_up_low   = low_tab(:,2);
E_mid_low  = low_tab(:,3);
E_lo_low   = low_tab(:,4);

zband      = 1.64;                    % ~90% CI
muE_low    = E_mid_low;               % mean emissions
sigmaE_low  = (E_up_low - E_lo_low) / (2*zband);
sigmaE_low(sigmaE_low <= 0) = 1e-6;

A_low    = muE_low;                   % allowance = mean emissions
Qmax_low = alpha * muE_low;           % max CCER usage

% 2.2 Normal-emission firms (Table 3)
% Columns: [Ticker, E_upper, E_mid, E_lower]
norm_tab = [ ...
 600011 9076451 8251319 7426187; ...
 600795 3927170 3570155 3213139; ...
 601991 5552259 5047508 4542757; ...
 600027 6756622 6142383 5528145; ...
 600023 3795945 3450859 3105773; ...
 539    2368211 2152919 1937627; ...
 600021 1540961 1400873 1260786; ...
 27     2276119 2069199 1862279; ...
 2608   2132345 1938495 1744646; ...
 600578 1708917 1553561 1398205; ...
 600575 1445654 1314231 1182808; ...
 600157 1533348 1393952 1254557; ...
 543    1126340 1023946 921551; ...
 600642 2127118 1933743 1740369; ...
 600863 584866 531697 478527; ...
 600    534253 485685 437116; ...
 767    1034726 940660 846594; ...
 966    723281 657528 591775; ...
 1896   782009 710918 639826; ...
 600780 425868 387153 348437; ...
 600509 583520 530472 477425; ...
 690    452755 411595 370436; ...
 600744 691180 628346 565511; ...
 899    170012 154556 139101; ...
 531    238187 216534 194881; ...
```

```
 600396 249379 226708 204037; ...
 2893   82005 74550 67095; ...
 600969 204230 185664 167098; ...
 791    95916 87197 78477; ...
 601    317822 288929 260036; ...
 600483 885339 804853 724368; ...
 883    1542108 1401917 1261725; ...
 600900 1554752 1413411 1272070; ...
 601985 3887484 3534076 3180668; ...
 600886 1218380 1107618 996856; ...
 601669 26125183 23750167 21375150];

ticker_norm = norm_tab(:,1);
E_up_norm   = norm_tab(:,2);
E_mid_norm  = norm_tab(:,3);
E_lo_norm   = norm_tab(:,4);

muE_norm    = E_mid_norm;
sigmaE_norm = (E_up_norm - E_lo_norm) / (2*zband);
sigmaE_norm(sigmaE_norm <= 0) = 1e-6;

A_norm    = muE_norm;
Qmax_norm = alpha * muE_norm;

%% 3. CCER marginal willingness-to-pay function (LaTeX-based)

pc_fun = @(Q, muE, sigmaE, A) ...
   v_res + (pA_bar - v_res) .* (1 - normcdf( (A + Q - muE) ./ sigmaE ));

phi = @(x) exp(-0.5*x.^2) ./ sqrt(2*pi);

%% 4. Merge samples and compute firm-level results

ticker_all = [ticker_low; ticker_norm];
muE_all    = [muE_low;  muE_norm];
sigma_all  = [sigmaE_low; sigmaE_norm];
A_all      = [A_low; A_norm];
Qmax_all   = [Qmax_low; Qmax_norm];

Nfirm       = numel(ticker_all);
Qstar_all   = zeros(Nfirm,1);
pC_Q0_all   = zeros(Nfirm,1);
pC_Qmax_all = zeros(Nfirm,1);
pC_Qstar_all = zeros(Nfirm,1);
```

```
% Representative firm: median mu_E
[~,idx_med] = min(abs(muE_all - median(muE_all)));
idx_rep     = idx_med;

nQgrid    = 50;
Qgrid_rep = linspace(0, Qmax_all(idx_rep), nQgrid);
pc_rep    = pc_fun(Qgrid_rep, muE_all(idx_rep), sigma_all(idx_rep), A_all(idx_rep));

fprintf('================ CCER Valuation (Firm-Level) ================\n');
fprintf('Global parameters:\n');
fprintf('  alpha     = %.4f (max CCER offset ratio)\n', alpha);
fprintf('  pA_bar    = %.2f CNY/t (expected marginal CEA settlement price)\n', pA_bar);
fprintf('  v_res     = %.2f CNY/t (residual value of CCER)\n\n', v_res);

fprintf('Firm-level parameters and key prices:\n');
fprintf('%-10s %-14s %-14s %-14s %-14s %-14s %-14s\n', ...
   'Ticker','mu_E','sigma_E','Qmax','pC(Q=0)','pC(Qmax)','pC(Q*)');

for i = 1:Nfirm
   muE_i  = muE_all(i);
   sig_i  = sigma_all(i);
   A_i    = A_all(i);
   Qmax_i = Qmax_all(i);

   % Marginal prices at Q=0 and Q=Qmax
   pC_Q0_all(i)    = pc_fun(0,      muE_i, sig_i, A_i);
   pC_Qmax_all(i)  = pc_fun(Qmax_i, muE_i, sig_i, A_i);

   % Optimal Q* by minimizing expected total cost
   obj = @(q) ETC_single(q, muE_i, sig_i, A_i, pA_bar, v_res, phi, @normcdf);
   [Qstar_i, ~] = fminbnd(obj, 0, Qmax_i);

   Qstar_all(i)    = Qstar_i;
   pC_Qstar_all(i) = pc_fun(Qstar_i, muE_i, sig_i, A_i);

   fprintf('%-10d %-14.2f %-14.2f %-14.2f %-14.2f %-14.2f %-14.2f\n', ...
      ticker_all(i), muE_i, sig_i, Qmax_i, ...
      pC_Q0_all(i), pC_Qmax_all(i), pC_Qstar_all(i));
end

%% 5. Weighted average theoretical CCER prices (mu_E weights)

weight       = muE_all / sum(muE_all);
avg_pC_Q0    = sum(weight .* pC_Q0_all);
avg_pC_Qmax  = sum(weight .* pC_Qmax_all);
```

```
avg_pC_Qstar  = sum(weight .* pC_Qstar_all);

fprintf('\nWeighted-average theoretical CCER prices (weights = mu_E):\n');
fprintf('  Mean p_C^*(Q=0)    = %.2f CNY/t\n', avg_pC_Q0);
fprintf('  Mean p_C^*(Q=Qmax) = %.2f CNY/t\n', avg_pC_Qmax);
fprintf('  Mean p_C^*(Q=Q*)   = %.2f CNY/t\n\n', avg_pC_Qstar);

%% 6. Explicit description of Figure 1 (representative firm)

rep_ticker      = ticker_all(idx_rep);
rep_muE         = muE_all(idx_rep);
rep_sigmaE      = sigma_all(idx_rep);
rep_A           = A_all(idx_rep);
rep_Qmax        = Qmax_all(idx_rep);
rep_Q0          = 0;
rep_Qstar       = Qstar_all(idx_rep);
rep_pC_Q0       = pC_Q0_all(idx_rep);
rep_pC_Qmax     = pC_Qmax_all(idx_rep);
rep_pC_Qstar    = pC_Qstar_all(idx_rep);

fprintf('Figure 1 (Representative firm p_C^*(Q) curve):\n');
fprintf('  Representative firm ticker           : %d\n', rep_ticker);
fprintf('  Representative firm mu_E             : %.2f t CO2\n', rep_muE);
fprintf('  Representative firm sigma_E          : %.2f t CO2\n', rep_sigmaE);
fprintf('  Representative firm allowance A      : %.2f t CO2\n', rep_A);
fprintf('  Representative firm Qmax             : %.2f t CO2\n', rep_Qmax);
fprintf('  Horizontal axis: Q in million t CO2 from %.2f to %.2f\n', ...
      rep_Q0/1e6, rep_Qmax/1e6);
fprintf('  Vertical axis: p_C^*(Q) in CNY/t\n');
fprintf('  Curve: p_C^*(Q) for Q in [0, Qmax]\n');
fprintf('  Horizontal reference line: p_A_bar  = %.2f CNY/t\n', pA_bar);
fprintf('  Horizontal reference line: v_res    = %.2f CNY/t\n', v_res);
fprintf('  Marked point at Q=0     : Q = %.2f,   p_C^*(0)    = %.2f CNY/t\n', ...
      rep_Q0, rep_pC_Q0);
fprintf('  Marked point at Q=Qmax   : Q = %.2f,   p_C^*(Qmax) = %.2f CNY/t\n', ...
      rep_Qmax, rep_pC_Qmax);
fprintf('  Marked point at Q=Q*     : Q* = %.2f,  p_C^*(Q*)   = %.2f CNY/t\n\n', ...
      rep_Qstar, rep_pC_Qstar);

%% 7. Explicit description of Figure 2 (distribution of p_C^*(Q*))

pC_min = min(pC_Qstar_all);
pC_max = max(pC_Qstar_all);
pC_mean = mean(pC_Qstar_all);
pC_median = median(pC_Qstar_all);
```

```
pC_std = std(pC_Qstar_all);

fprintf('Figure 2 (Distribution of firm-level optimal marginal CCER prices p_C^*(Q*)):\n');
fprintf('  Sample size (number of firms)       : %d\n', Nfirm);
fprintf('  Horizontal axis: p_C^*(Q*) in CNY/t\n');
fprintf('  Vertical axis: number of firms (histogram counts)\n');
fprintf('  Range of p_C^*(Q*)                  : [%.2f, %.2f] CNY/t\n', pC_min, pC_max);
fprintf('  Mean   of p_C^*(Q*)                 : %.2f CNY/t\n', pC_mean);
fprintf('  Median of p_C^*(Q*)                 : %.2f CNY/t\n', pC_median);
fprintf('  Std. deviation of p_C^*(Q*)         : %.2f CNY/t\n\n', pC_std);

%% 8. Figures (two figures only)

% Figure 1: Representative firm p_C^*(Q) curve
figure;
plot(Qgrid_rep/1e6, pc_rep, 'b-', 'LineWidth', 2); hold on;
yline(pA_bar,'r--','LineWidth',1.5);
yline(v_res,'k-.','LineWidth',1.5);
xlabel('Q (million t CO_2)');
ylabel('p_C^*(Q) (CNY/t)');
title(sprintf('Representative Firm (Ticker=%d): p_C^*(Q)', rep_ticker));
legend('p_C^*(Q)','p_A^{bar}','v_{res}','Location','best');
grid on;

plot(rep_Q0/1e6, rep_pC_Q0,'ko','MarkerFaceColor','k');
text(rep_Q0/1e6, rep_pC_Q0, '  Q=0','VerticalAlignment','bottom');

plot(rep_Qmax/1e6, rep_pC_Qmax, 'ko','MarkerFaceColor','k');
text(rep_Qmax/1e6, rep_pC_Qmax, '  Q=Q_{max}','VerticalAlignment','top');

plot(rep_Qstar/1e6, rep_pC_Qstar, 'ro','MarkerFaceColor','r');
text(rep_Qstar/1e6, rep_pC_Qstar, '  Q=Q^*','VerticalAlignment','bottom');

% Figure 2: Distribution of optimal marginal CCER prices p_C^*(Q*)
figure;
histogram(pC_Qstar_all, 'FaceColor',[0.2 0.6 0.8]);
xlabel('p_C^*(Q^*) (CNY/t)');
ylabel('Number of firms');
title('Distribution of Firm-Level Optimal CCER Marginal Prices');
grid on;

%% 9. Auxiliary function: expected total cost for a single firm

function ETC = ETC_single(Q, muE, sigmaE, A, pA_bar, v_res, phi, normcdf_handle)
   T    = A + Q;
```

```
    a     = (T - muE) ./ sigmaE;
    Phi_a = normcdf_handle(a);
    phi_a = phi(a);

    E_gap_pos     = sigmaE .* (phi_a - a .* (1 - Phi_a)); % E[(E - T)_+]
    E_surplus_pos = sigmaE .* (phi_a + a .* Phi_a);       % E[(T - E)_+]

    pC_star = v_res + (pA_bar - v_res) .* (1 - Phi_a);

    ETC = pC_star .* Q + pA_bar .* E_gap_pos - v_res .* E_surplus_pos;
end
```

Appendix C

```
function main_regime_switching_CCER_smooth_v2
clc; clear; close all;

CEA_2023 = [ ...
138.00 110.40 90.00 72.00 59.00 51.47 61.80 74.20 74.20 74.20 ...
89.00 74.00 106.80 86.00 102.00 115.64 138.50 111.00 92.22 73.80 75.00 ...
88.77 106.60 125.00 149.64 144.30 131.75 134.00 124.00 100.90 121.00 ...
130.12 139.00 127.00 127.00 121.77 142.00 121.88 127.00 120.00 130.00 ...
127.00 130.00 132.53 122.50 133.50 128.00 128.00 123.03 124.00 127.50 ...
119.18 123.57 123.77 121.28 123.00 130.29 121.35 115.13 125.25 124.94 ...
124.17 127.93 125.17 121.38 117.72 126.25 123.03 116.89 105.28 120.71 ...
118.88 118.44 121.37 124.41 113.92 119.90 115.96 119.96 113.01 109.92 ...
118.49 109.91 108.16 121.72 116.00 103.32 100.00 110.00 109.00 110.00 ...
114.34 95.00 85.06 102.00 107.00 115.00 116.00 112.00 111.38]';

CCER_2023 = [ ...
95.00 95.00 95.00 109.00 88.00 80.00 90.00 90.89 47.00 78.00 ...
80.00 80.00 56.40 90.00 80.00 82.00 80.00 80.00 80.00 80.34 80.00 75.00 ...
80.00 80.00 86.96 80.00 80.01 84.81 88.00 65.64 80.00 69.70 81.40 80.00 ...
69.38 70.50 80.44 83.90 78.23 86.00 86.99 80.00 80.00 74.77 77.63 74.50 ...
75.00 80.10 85.40 80.00 74.00 70.42 78.00 79.51 79.14 85.00 80.00 75.00 ...
65.00 65.00 74.60 65.01 70.00 90.00 70.00 72.00 72.00 72.00]';

n_days = length(CEA_2023);

g_yoy = [ ...
2.0  ;
5.8  ;
5.9  ;
8.3  ;
7.4  ;
6.4  ;
```

```
6.5  ;
7.6  ;
6.8  ;
5.2  ;
11.6 ;
8.0  ];
g_yoy = g_yoy / 100;

month_id = zeros(n_days,1);
edges = round(linspace(1, n_days+1, 13));
for m = 1:12
   month_id(edges(m):edges(m+1)-1) = m;
end
elec_yoy_daily = g_yoy(month_id);

q_elec  = quantile(elec_yoy_daily, [0.33 0.66]);
q_price = quantile(CEA_2023,       [0.33 0.66]);
elec_low  = q_elec(1);
elec_high = q_elec(2);
p_low     = q_price(1);
p_high    = q_price(2);

state = zeros(n_days,1);

for t = 1:n_days
   e = elec_yoy_daily(t);
   p = CEA_2023(t);
   if (e <= elec_low && p <= p_low)
      state(t) = 1;
   elseif (e >= elec_high && p >= p_high)
      state(t) = 3;
   else
      state(t) = 2;
   end
end

for s = 1:3
   if sum(state==s) < 5
      warning('State %d has too few observations, merging to middle state.', s);
      state(state==s) = 2;
   end
end

log_ret_CEA = diff(log(CEA_2023));
state_ret   = state(2:end);
```

```
n_state    = 3;
mu_A       = zeros(n_state,1);
sig_A      = zeros(n_state,1);

for s = 1:n_state
   idx = (state_ret == s);
   rs  = log_ret_CEA(idx);
   if isempty(rs)
      rs = log_ret_CEA;
   end
   mu_A(s)  = mean(rs);
   sig_A(s) = std(rs);
end

theta_daily = CCER_2023 ./ CEA_2023(1:length(CCER_2023));
state_theta = state(1:length(theta_daily));

theta_state = zeros(n_state,1);
for s = 1:n_state
   idx = (state_theta == s);
   ths = theta_daily(idx);
   if isempty(ths)
      ths = theta_daily;
   end
   theta_state(s) = mean(ths);
end
theta_state = max(theta_state, 0.5);
theta_state = min(theta_state, 1.0);

P = zeros(n_state);
for s = 1:n_state
   idx = find(state(1:end-1) == s);
   if isempty(idx)
      P(s,:) = 1/n_state;
   else
      next_s = state(idx+1);
      for j = 1:n_state
         P(s,j) = sum(next_s == j);
      end
      P(s,:) = P(s,:) / sum(P(s,:));
   end
end

A_pi = [ (P' - eye(n_state)); ones(1,n_state) ];
b_pi = [ zeros(n_state,1); 1 ];
```

```
pi_stationary = A_pi \ b_pi; %#ok<NASGU>

r_annual = 0.0435;
T_trade  = 80;
dt       = 1/252;
r_dt     = r_annual * dt;

S0_CEA  = CEA_2023(end);
S0_CCER = CCER_2023(end);
K       = S0_CCER;

n_paths = 20000;

n_plot = 5;
CEA_path_plot    = zeros(T_trade+1, n_plot);
CCER_path_plot   = zeros(T_trade+1, n_plot);
Regime_path_plot = zeros(T_trade+1, n_plot);

payoff = zeros(n_paths,1);

rng(1234);

for pidx = 1:n_paths
   cur_s = state(end);
   S_A   = S0_CEA;
   S_C   = S0_CCER;

   if pidx <= n_plot
      CEA_path_plot(1,pidx)     = S_A;
      CCER_path_plot(1,pidx)    = S_C;
      Regime_path_plot(1,pidx)  = cur_s;
   end

   for t = 1:T_trade
      cur_s = draw_next_state(cur_s, P);
      sig   = sig_A(cur_s);
      dW    = sqrt(dt)*randn;
      mu_rn = r_annual - 0.5*sig^2;
      S_A   = S_A * exp(mu_rn*dt + sig*dW);
      theta = theta_state(cur_s);
      eps_c = 0.10*sqrt(dt)*randn;
      S_C   = theta * S_A * exp(eps_c);

      if pidx <= n_plot
         CEA_path_plot(t+1,pidx)    = S_A;
```

```
        CCER_path_plot(t+1,pidx)   = S_C;
        Regime_path_plot(t+1,pidx) = cur_s;
      end
   end
   payoff(pidx) = max(S_C, K);
end

PV_CCER_value = exp(-r_dt*T_trade) * mean(payoff);

time_vec = 0:T_trade;

figure('Name','Regime-switching GBM: CEA/CCER sample paths','Color','w','Position',[100 100 900 420]);
hold on;

for i = 1:n_plot
   plot(time_vec, CEA_path_plot(:,i), '-','LineWidth',1.4,'Color',[0 0.447 0.741]);
   plot(time_vec, CCER_path_plot(:,i),'--','LineWidth',1.4,'Color',[0.85 0.325 0.098]);
end

ymax_all = max( [CEA_path_plot(:); CCER_path_plot(:)] );
ymin_all = min( [CEA_path_plot(:); CCER_path_plot(:)] );
ylim([ymin_all*0.98, ymax_all*1.02]);

reg_path = Regime_path_plot(:,1);

colors = [0.9 0.95 1.0;
        0.9 1.0 0.9;
        1.0 0.9 0.9];

for t = 1:T_trade
   s = reg_path(t);
   x_rect = [t-0.5, t+0.5, t+0.5, t-0.5];
   y_rect = [ymin_all*0.98, ymin_all*0.98, ymax_all*1.02, ymax_all*1.02];
   patch(x_rect, y_rect, colors(s,:), 'EdgeColor','none','FaceAlpha',0.18);
end

for i = 1:n_plot
   plot(time_vec, CEA_path_plot(:,i), '-','LineWidth',1.4,'Color',[0 0.447 0.741]);
   plot(time_vec, CCER_path_plot(:,i),'--','LineWidth',1.4,'Color',[0.85 0.325 0.098]);
end

xlabel('Trading day');
ylabel('Price (CNY)');
title('Sample paths of CEA (solid) and CCER (dashed) under regime-switching GBM');
grid on;
```

```
xlim([0 T_trade]);
legend({'CEA paths','CCER paths'},'Location','northwest');

hold off;

S0_grid = linspace(80, 160, 25);
T_grid  = 10:10:80;
nS = length(S0_grid);
nT = length(T_grid);

n_path_small = 15000;

K_base     = CCER_2023(end);
theta_mid  = theta_state(2);
alpha_follow = 0.3;

rng(5678);

S_samples = zeros(nS*nT,1);
T_samples = zeros(nS*nT,1);
P_samples = zeros(nS*nT,1);
idx_sample = 0;

for iT = 1:nT
   TT   = T_grid(iT);
   disc = exp(-r_dt*TT);
   for iS = 1:nS
      idx_sample = idx_sample + 1;
      S0a = S0_grid(iS);
      K2  = K_base + alpha_follow * theta_mid * (S0a - S0_CEA);
      payoff2 = zeros(n_path_small,1);
      for pidx = 1:n_path_small
         cur_s = state(end);
         Sa    = S0a;
         Sc    = theta_state(cur_s) * Sa;
         for t = 1:TT
            cur_s = draw_next_state(cur_s, P);
            sig   = sig_A(cur_s);
            dW    = sqrt(dt)*randn;
            mu_rn = r_annual - 0.5*sig^2;
            Sa    = Sa * exp(mu_rn*dt + sig*dW);
            theta = theta_state(cur_s);
            eps_c2 = 0.10*sqrt(dt)*randn;
            Sc     = theta * Sa * exp(eps_c2);
         end
```

```
        ScT = Sc;
        payoff2(pidx) = max(ScT, K2);
      end
      price_ij = disc * mean(payoff2);
      S_samples(idx_sample) = S0a;
      T_samples(idx_sample) = TT;
      P_samples(idx_sample) = price_ij;
   end
end

[SG_orig, TG_orig] = meshgrid(S0_grid, T_grid);
Price_surface = griddata(S_samples, T_samples, P_samples, SG_orig, TG_orig, 'linear');

figure('Name','CCER value surface: discounted E[max(CCER_T, K2)] (no extra smoothing)',...
     'Color','w','Position',[150 150 900 620]);

surf(SG_orig, TG_orig, Price_surface);
xlabel('Initial CEA price S_0^A (CNY)','FontSize',11);
ylabel('Maturity T (trading days)','FontSize',11);
zlabel('Discounted E[ max(CCER_T, K_2) ] (CNY)','FontSize',11);
title('CCER value surface under regime-switching GBM: discounted E[max(CCER_T, K_2)]','FontSize',12);
shading interp;
colormap(parula);
colorbar;
grid on;
view(135, 30);

hold on;
[~, idx_T40] = min(abs(T_grid - 40));
plot3(S0_grid, T_grid(idx_T40)*ones(1,nS), Price_surface(idx_T40,:), ...
    'k-','LineWidth',2);
text(S0_grid(end), T_grid(idx_T40), Price_surface(idx_T40,end), ...
   '  Slice at T \approx 40','Color','k','FontSize',10);
hold off;

fprintf('================ Regime-Switching CCER Valuation (E[max(CCER_T, K)]) ================\n');
fprintf('Risk-free annual rate r     : %.4f\n', r_annual);
fprintf('Simulation horizon (T_trade): %d trading days\n', T_trade);
fprintf('Time step dt (in years)     : 1/252\n\n');

fprintf('--- Figure 1: Sample paths under regime-switching GBM ---\n');
fprintf('Initial CEA price S0^A      : %.2f CNY\n', S0_CEA);
fprintf('Initial CCER price S0^C     : %.2f CNY\n', S0_CCER);
fprintf('Regimes (1=low, 2=mid, 3=high) are inferred from 2023 data.\n');
fprintf('The figure shows %d simulated CEA (solid) and CCER (dashed) paths,\n', n_plot);
```

```
fprintf('with colored background bands indicating regime switches over time.\n');
fprintf('These paths illustrate how CCER prices co-move with CEA prices\n');
fprintf('and how different regimes (low/medium/high demand and price) affect\n');
fprintf('the joint evolution of the two carbon assets.\n\n');

fprintf('--- Single-maturity CCER value at T = %d trading days ---\n', T_trade);
fprintf('Guarantee level K (per unit CCER)        : %.2f CNY\n', K);
fprintf('Number of Monte Carlo paths (T = %d)     : %d\n', T_trade, n_paths);
fprintf('Discounted E[ max(CCER_T, K) ] (per unit) : %.4f CNY\n\n', PV_CCER_value);

fprintf('--- Figure 2: CCER value surface on the original (S0^A, T) grid ---\n');
fprintf('Grid of initial CEA prices S0^A          : from %.2f to %.2f CNY (%d points)\n', ...
    min(S0_grid), max(S0_grid), nS);
fprintf('Grid of maturities T                     : from %d to %d trading days (%d points)\n', ...
    min(T_grid), max(T_grid), nT);
fprintf('Monte Carlo paths per (S0^A, T) grid point: %d\n', n_path_small);
fprintf('K2 is defined as K_base + alpha_follow * theta_mid * (S0^A - S0_CEA),\n');
fprintf('where K_base = %.2f, alpha_follow = %.2f, theta_mid = %.4f.\n', ...
    K_base, alpha_follow, theta_mid);
fprintf('This breaks the nearly linear dependence on S0^A while preserving\n');
fprintf('the overall guarantee-contract structure E[max(CCER_T, K2)].\n');
fprintf('The 3D surface is plotted directly on this original grid without\n');
fprintf('any additional smoothing beyond the basic griddata interpolation.\n');
fprintf('================================================================================\n');

end

function next_s = draw_next_state(cur_s, P)
prob = P(cur_s,:);
u = rand;
cumprob = cumsum(prob);
next_s = find(u <= cumprob, 1, 'first');
if isempty(next_s)
   next_s = cur_s;
end
end
```